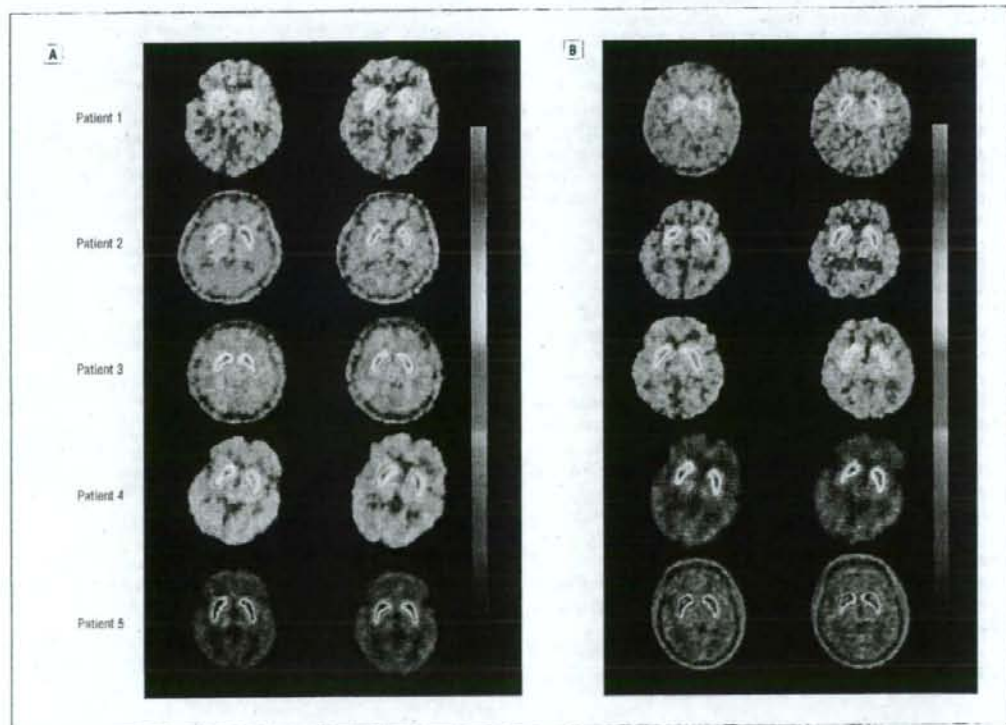


**Table 3. Positron Emission Tomography (PET) and Single-Photon Emission Computed Tomography (SPECT) Findings of 5 Patients**

Patient	PET Striatum	<sup>18</sup> F-L-dopa		NMSP		SPECT	
		Left	Right	Left	Right	Cortex	Basal Ganglia
1	Ventral	2.13	2.15	3.73	3.85	Blood flow decreased in areas 4, 6, 8, 10, and in the right cerebellar hemisphere.	Blood flow decreased in the bilateral corpus striatum.
	Intermediate	2.18	2.10	3.78	3.94		
	Dorsal	2.00	1.94	3.40	3.37		
2	Ventral	3.03	3.20	4.09	4.53	Blood flow decreased in the frontal lobe (greater decrease in the right frontal lobe) and in the left cerebellar hemisphere.	Blood flow decreased in the right corpus striatum and in the right thalamus.
	Intermediate	3.20	3.00	4.46	4.70		
	Dorsal	2.96	2.58	3.90	4.09		
3	Ventral	2.49	2.69	4.23	4.25	Blood flow decreased in the bilateral frontal lobe (especially area 6) and in the bilateral temporoparietal lobe.	Normal.
	Intermediate	2.62	2.69	4.23	4.25		
	Dorsal	2.40	2.39	3.70	3.86		
4	Ventral	2.15	2.23	4.31	4.18	Normal	Blood flow decreased in the left basal ganglia.
	Intermediate	2.46	2.40	4.44	4.60		
	Dorsal	2.24	2.31	3.79	4.12		
5	Ventral	2.85	2.90	3.23	3.31	Blood flow decreased in the right temporal occipital parietal lobe.	Blood flow decreased in the left basal ganglia.
	Intermediate	3.05	3.10	3.82	3.56		
	Dorsal	2.41	2.56	3.18	3.16		

Abbreviation: NMSP, [<sup>11</sup>C]N-methylspiperone.



**Figure.** Positron emission tomography images of study patients. A, <sup>18</sup>F-L-dopa images. B, <sup>11</sup>C-N-methylspiperone images. Two adjacent sections including the basal ganglia are shown.

the number of neurons in the substantia nigra; Lewy bodies were rarely reported.<sup>8</sup> These lines of evidence suggest that parkinsonism in ALS is not likely an association of Parkinson disease with ALS, but is likely due to pathological changes in areas other than the substantia nigra.

In this context, it is worth noting that isolated lesions in the supplementary motor area are associated with clinical features very similar to parkinsonism, dominated by severe akinesia and mild rigidity without resting tremor.<sup>7</sup> Regional cerebral blood flow has been reported to be decreased in the frontal cortices, including the supplementary motor area of patients with Parkinson disease; however, flow could be reversed with anti-parkinsonian treatment.<sup>8</sup> Thus, clinical manifestations quite similar to parkinsonism can be produced by isolated cortical lesions in the supplementary motor area. Reduction of regional cerebral blood flow in the frontal and/or temporal cortices extending beyond the primary motor area has been demonstrated in both ALS with dementia and classic ALS without dementia.<sup>9</sup> This observation is in accordance with our single-photon emission computed tomography scan results showing 4 patients with a decrease of regional cerebral blood flow in the frontal and/or temporal cortices.

The degree of regional cerebral blood flow reduction in the frontal and anterior temporal lobes has been reported to correlate with severity of dementia in ALS patients with associated dementia; these blood flow characteristics are indistinguishable from those seen in patients with frontotemporal dementia.<sup>10</sup> Indeed, ALS is not infrequently (approximately 15% of cases) associated with frontotemporal dementia, and involvement of lower motor neurons was found in a group of patients with frontotemporal dementia without a prior diagnosis of ALS.<sup>11</sup> A subclass of frontotemporal dementia with tau negative and ubiquitin-positive inclusions has been classified as frontotemporal lobar degeneration with motor neuron disease (FTLD-MND) and frontotemporal lobar degeneration with motor neuron disease type (FTLD-MND type), respectively, depending on the presence or absence of clinically overt motor neuron signs.<sup>12</sup> These diagnostic subclasses (FTLD-MND and FTLD-MND type) have been reported to comprise 40% of pathologically proven frontotemporal dementia cases. In addition, patients with frontotemporal dementia frequently exhibit parkinsonism, but neuropathological changes in the substantia nigra were more marked in patients with concomitant dementia irrespective of the presence or absence of parkinsonism, as compared with patients without dementia<sup>13</sup>; hence, reduction of nigrostriatal dopaminergic function may not be associated with parkinsonism. Common pathological changes have been demonstrated in FTLD-MND, FTLD-MND type, and classic ALS without dementia, implying that these diseases comprise a clinicopathological spectrum rather than individual entities.<sup>13</sup>

Taken together, parkinsonism associated with ALS or FTLD-MND may not be due to a dysfunction of the ni-

grostriatal dopaminergic neurons but rather frontal lesions including the supplementary motor area.

Accepted for Publication: May 30, 2006.

Correspondence: Takuto Hideyama, MD, 7-3-1 Hongo, Bunkyo-Ku, Tokyo 113-8655, Japan (hideyama-int@u-tokyo.ac.jp).

Author Contributions: *Study concept and design:* Hideyama and Kwak. *Acquisition of data:* Hideyama, Momose, Shimizu, Tsuji, and Kwak. *Analysis and interpretation of data:* Hideyama, Momose, Shimizu, Tsuji, and Kwak. *Drafting of the manuscript:* Hideyama, Momose, Shimizu, Tsuji, and Kwak. *Critical revision of the manuscript for important intellectual content:* Hideyama, Momose, Shimizu, Tsuji, and Kwak. *Statistical analysis:* Hideyama. *Obtained funding:* Kwak. *Administrative, technical, and material support:* Hideyama, Momose, Shimizu, Tsuji, and Kwak. *Study supervision:* Momose, Shimizu, Tsuji, and Kwak.

Financial Disclosure: None reported.

Acknowledgment: We are grateful to Dr Shigeo Murayama for valuable discussion and for the efforts of the young neurologists in our department.

## REFERENCES

1. Eisen A, Calne D. Amyotrophic lateral sclerosis, Parkinson's disease and Alzheimer's disease: phylogenetic disorders of the human neocortex sharing many characteristics. *Can J Neurol Sci.* 1992;19(1 Suppl):117-123.
2. Williams TL, Shaw PJ, Lowe J, Bates D, Ince PG. Parkinsonism in motor neuron disease: case report and literature review. *Acta Neuropathol (Berl).* 1995;89:275-283.
3. Takahashi H, Snow BJ, Bhatt MH, Peppard R, Eisen A, Calne DB. Evidence for a dopaminergic deficit in sporadic amyotrophic lateral sclerosis on positron emission scanning. *Lancet.* 1993;342:1016-1018.
4. Brooks BR. Versailles minimal dataset for diagnosis of ALS: a distillate of the 2nd Consensus Conference on accelerating the diagnosis of ALS. Versailles 2nd Consensus Conference participants. *Amyotroph Lateral Scler Other Motor Neuron Disord.* March 2000;(suppl 1):S79-S81.
5. Yoshimura M, Yamamoto T, Iso-o N, et al. Hemiparkinsonism associated with a mesencephalic tumor. *J Neurol Sci.* 2002;197:89-92.
6. Yoshida M. Amyotrophic lateral sclerosis with dementia: the clinicopathological spectrum. *Neuropathology.* 2004;24:87-102.
7. Dick JP, Benecke R, Rothwell JC, Day BL, Marsden CD. Simple and complex movements in a patient with infarction of the right supplementary motor area. *Mov Disord.* 1986;1:255-266.
8. Jenkins IH, Fernandez W, Playford ED, et al. Impaired activation of the supplementary motor area in Parkinson's disease is reversed when akinesia is treated with apomorphine. *Ann Neurol.* 1992;32:749-757.
9. Abrahams S, Goldstein LH, Kew JJ, et al. Frontal lobe dysfunction in amyotrophic lateral sclerosis: a PET study. *Brain.* 1996;119:2105-2120.
10. Verclletto M, Ronin M, Huvel M, Maigne C, Feve JR. Frontal type dementia preceding amyotrophic lateral sclerosis: a neuropsychological and SPECT study of five clinical cases. *Eur J Neurol.* 1999;6:295-299.
11. Lomen-Hoerth C, Anderson T, Miller B. The overlap of amyotrophic lateral sclerosis and frontotemporal dementia. *Neurology.* 2002;59:1077-1079.
12. McKhann GM, Albert MS, Grossman M, Miller B, Dickson D, Trojanowski JQ. Clinical and pathological diagnosis of frontotemporal dementia: report of the Work Group on Frontotemporal Dementia and Pick's Disease. *Arch Neurol.* 2001;58:1803-1809.
13. Mackenzie IR, Feldman H. The relationship between extramotor ubiquitin-immunoreactive neuronal inclusions and dementia in motor neuron disease. *Acta Neuropathol (Berl).* 2003;105:98-102.





## Calcium-permeable AMPA channels in neurodegenerative disease and ischemia

Shin Kwak<sup>1</sup> and John H Weiss<sup>2</sup>

Compelling evidence supports contributions of glutamate receptor overactivation ('excitotoxicity') to neurodegeneration in both acute conditions, such as stroke, and chronic neurodegenerative conditions, such as amyotrophic lateral sclerosis. However, anti-excitotoxic therapeutic trials, which have generally targeted highly  $\text{Ca}^{2+}$  permeable NMDA-type glutamate channels, have to date failed to demonstrate impressive efficacy. Whereas most AMPA type glutamate channels are  $\text{Ca}^{2+}$  impermeable, an evolving body of evidence supports the contention that relatively unusual  $\text{Ca}^{2+}$  permeable AMPA channels might be crucial contributors to injury in these conditions. These channels are preferentially expressed in discrete neuronal subpopulations, and their numbers appear to be upregulated in amyotrophic lateral sclerosis and stroke. In addition, unlike NMDA channels,  $\text{Ca}^{2+}$  permeable AMPA channels are not blocked by  $\text{Mg}^{2+}$ , but are highly permeable to another potentially harmful endogenous cation,  $\text{Zn}^{2+}$ . The targeting of these channels might provide efficacious new avenues in the therapy of certain neurological diseases.

### Addresses

<sup>1</sup> Department of Neurology, Graduate School of Medicine, University of Tokyo, 7-3-1 Hongo, Bunkyo-ku, 113-8655 Tokyo, Japan  
<sup>2</sup> 2101 Gillespie Building, University of California, Irvine, CA 92697-4292, USA

Corresponding author: Weiss, John H (jweiss@uci.edu)

Current Opinion in Neurobiology 2006, 16:281-287

This review comes from a themed issue on  
Signalling mechanisms  
Edited by Erin M Schuman and Peter H Seeburg

Available online 15th May 2006

0959-4388/\$ - see front matter  
© 2006 Elsevier Ltd. All rights reserved.

DOI 10.1016/j.conb.2006.05.004

### Introduction

Excessive extracellular exposure to glutamate, an excitatory neurotransmitter, is harmful to neurons and contributes to neurodegeneration in certain diseases of the central nervous system. In amyotrophic lateral sclerosis (ALS), toxic elevations of glutamate appear to result from loss or dysfunction of astrocytic glutamate transporters. In ischemia, rapid glutamate release combined with deficiency in (or even reversal of) uptake causes extracellular glutamate accumulation.

Glutamate activates a number of types of postsynaptic ion channels. Most prominent among these are NMDA (N-

methyl-D-aspartic acid)-type glutamate channels, which are highly  $\text{Ca}^{2+}$  permeable, and AMPA (1-amino-3-hydroxy-5-methyl-4-isoxazole propionic acid)-type glutamate channels, which mediate most rapid excitatory neurotransmission and are generally  $\text{Ca}^{2+}$  impermeable. However, some AMPA channels are  $\text{Ca}^{2+}$  permeable and emerging evidence supports the idea that these unusual channels, which are preferentially expressed on discrete populations of neurons, might be crucial contributors to injury in both ALS and ischemia.

It is also apparent that the number of  $\text{Ca}^{2+}$  permeable AMPA channels is subject to regulation both in response to physiological patterns of synaptic activity and in certain pathological states. Specifically, whereas relatively few  $\text{Ca}^{2+}$  permeable AMPA channels are normally present on hippocampal pyramidal neurons (HPNs), the number of these channels can increase sharply after ischemia. By contrast, the motor neurons (MNs), which selectively degenerate in ALS, normally do possess substantial numbers of  $\text{Ca}^{2+}$  permeable AMPA channels. However, recent evidence suggests that the number of these channels might further increase in ALS. In this review, we discuss recent evidence for roles of  $\text{Ca}^{2+}$  permeable AMPA channels in disease, with particular emphasis on intriguing clues to their roles in ALS and ischemia.

### What are $\text{Ca}^{2+}$ -permeable AMPA channels, and how are they regulated?

Functional AMPA receptors are homo- or hetero-oligomeric assemblies that are composed of various combinations of four possible subunits, GluR1, GluR2, GluR3 and GluR4. The  $\text{Ca}^{2+}$  conductance of AMPA receptors differs markedly according to whether the GluR2 subunit is present or not. AMPA receptors that contain at least one GluR2 subunit have low  $\text{Ca}^{2+}$  conductance, whereas those lacking a GluR2 subunit are  $\text{Ca}^{2+}$  permeable [1]. These properties of GluR2 are generated post-transcriptionally by RNA editing at the Q/R site in the putative second membrane domain (M2), during which a glutamine (Q) codon is replaced by an arginine (R) codon [1]. The presence of this positively charged residue, the arginine, in the pore of the channel impedes  $\text{Ca}^{2+}$  permeation (Figure 1). Analyses of the RNA from adult rat, mouse, and human brains have demonstrated that almost all GluR2 mRNA in neurons is edited, whereas in the GluR1, GluR3 and GluR4 subunits glutamine remains at this crucial position. AMPA receptors containing an unedited GluR2 (GluR2Q) have high  $\text{Ca}^{2+}$  permeability [1,2].

**Glossary**

**Permeability transition pore:** A large conductance channel through the mitochondrial membranes, persistent opening of which has been associated with mitochondrial disruption, release of the apoptotic mediator, cytochrome C, and cell death.

**Ventral root avulsion:** An injury causing disruption of the connection among spinal motor neurons, which send their axons out of the spinal cord through the ventral root, and the muscles that they innervate.

Under normal circumstances, most neurons have few  $\text{Ca}^{2+}$  permeable AMPA channels, reflecting the presence of edited GluR2 subunits and, therefore, arginine impeding  $\text{Ca}^{2+}$  entry in most of their AMPA channels. Furthermore, AMPA channels are not static, but undergo dynamic regulation through many mechanisms. Levels of  $\text{Ca}^{2+}$  permeable AMPA channels can be regulated by alterations in receptor trafficking, and a decrease in the number of these channels can occur in response to physiological activation [3], through mechanisms that appear to be dependent upon specific protein-protein interactions with GluR2 [4,5]. Indicating the importance of such regulation, insertion of AMPA channels into the synaptic membrane is sensitive to the editing state of the GluR2 Q/R site [6,7]. In contrast to the studies in which physiological activation results in a decrease in the number of postsynaptic  $\text{Ca}^{2+}$  permeable AMPA channels, recent studies have found that the presence of tumor necrosis factor- $\alpha$  (TNF- $\alpha$ ), a cytokine, can result in membrane insertion of  $\text{Ca}^{2+}$  permeable AMPA channels in some neurons. This mechanism might promote neuronal injury in pathological conditions associated with

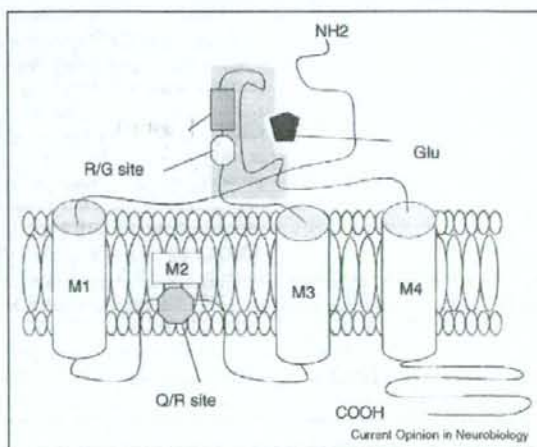
elevations of this cytokine [8,9,10]. As discussed below, the number of  $\text{Ca}^{2+}$  permeable AMPA channels can also be regulated at the level of GluR2 mRNA expression, as is hypothesized to be the case in ischemia [11,12], or by defects in mRNA editing, as is hypothesized to be the case in ALS [13,14,15].

### How might $\text{Ca}^{2+}$ permeable AMPA channel activation injure neurons?

Although mechanisms of excitotoxic neuronal injury are complex and not completely understood, intracellular  $\text{Ca}^{2+}$  overload is an important trigger. With substantial intracellular  $\text{Ca}^{2+}$  loading,  $\text{Ca}^{2+}$  is taken up into mitochondria, and can cause generation of reactive oxygen species (ROS) or opening of the permeability transition pore (see glossary) and release of apoptotic mediators such as cytochrome C. With more modest intracellular  $\text{Ca}^{2+}$  accumulation, injury could be mediated by other mechanisms, including generation of nitric oxide (NO), with consequent activation of poly(ADP-ribose) polymerase (PARP) and release of mitochondrial apoptosis inducing factor (AIF) [16].

Another way in which  $\text{Ca}^{2+}$  permeable AMPA channels might mediate injury is by serving as entry routes for the divalent cation,  $\text{Zn}^{2+}$ , which is co-released with glutamate at certain excitatory synapses.  $\text{Zn}^{2+}$  accumulates in HPNs in ischemia and epilepsy, both conditions in which  $\text{Zn}^{2+}$  chelators are neuroprotective [17,18]. Whereas the  $\text{Zn}^{2+}$  accumulation is probably due to a combination of 'translocation' across the synapse and mobilization from

Figure 1



Structure of an AMPA receptor subunit (GluR2). The Q/R site is localized in the P-loop or putative second membrane domain (M2), which faces the channel pore of the AMPA receptor. Permeation of divalent cations is prevented when positively charged arginine (R) is placed in the Q/R site (through editing of the GluR2 mRNA), but can permeate when neutral glutamine (Q) is present. Reprinted with permission from Figure 1b in Nishimoto *et al.* [50].



intracellular pools [18],  $\text{Ca}^{2+}$  permeable AMPA channels are highly  $\text{Zn}^{2+}$  permeable, and might thus be the primary route for entry of synaptic  $\text{Zn}^{2+}$  [19–21]. Similar to  $\text{Ca}^{2+}$ ,  $\text{Zn}^{2+}$  appears to induce injury through a number of mechanisms, including enzyme induction, ROS generation and PARP activation [22]. Intriguingly, however, in comparison to  $\text{Ca}^{2+}$ ,  $\text{Zn}^{2+}$  is far more potent at inducing disruption of mitochondrial function, raising the possibility that mitochondrial effects contribute prominently to the degeneration resulting from strong intracellular  $\text{Zn}^{2+}$  accumulation [20,23–25].

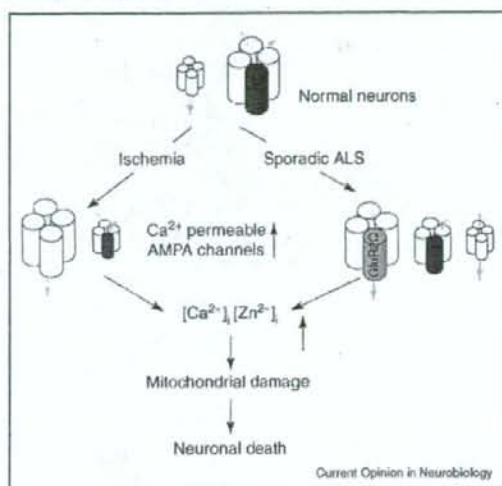
There are several reasons that  $\text{Ca}^{2+}$  permeable AMPA channels might be expected to play greater roles in neurodegeneration than NMDA channels. First, an increase in their number, as appears to happen in sporadic ALS and ischemia, would subject neurons to new metabolic burdens, possibly tipping the balance towards degeneration. Second, because NMDA channels are subject to voltage-dependent block by  $\text{Mg}^{2+}$  ions, they permit little  $\text{Ca}^{2+}$  entry in the absence of strong post-synaptic depolarization. Finally, the high  $\text{Zn}^{2+}$  permeability of  $\text{Ca}^{2+}$  permeable AMPA channels does not apply to NMDA channels, which are blocked by  $\text{Zn}^{2+}$ .

### Role in amyotrophic lateral sclerosis

An excitotoxic model of ALS was supported by the observation that astrocytic glutamate uptake is deficient in the motor cortices and spinal cords of ALS patients [26]. Furthermore, the finding that MNs are selectively vulnerable to injury caused by AMPA/kainate receptor activation [27,28] suggested a crucial role for these receptors. This vulnerability is possibly caused by the fact that MNs possess substantial numbers of  $\text{Ca}^{2+}$  permeable AMPA channels [27,29,30], a finding consistent with the observation that MNs possess a lower relative abundance of GluR2 mRNA as compared with that in other neuronal subclasses both in humans [31] and in rats [32].

If  $\text{Ca}^{2+}$  permeable AMPA channels play a crucial role in excitotoxic MN injury, an increase in their number might initiate or accelerate the disease. Recent studies using real-time reverse transcriptase-polymerase chain reaction (RT-PCR) to compare GluR2 mRNA expression between ALS patients and controls found no differences in total GluR2 mRNA levels or the ratio of GluR2 mRNA to total AMPA receptor subunit mRNA [31]. However, these studies did find evidence for a reduction of GluR2 editing efficiency [13\*\*,14\*,15], which appeared to be selective for MNs [13\*\*]. Furthermore, the editing defect appeared to be specific to ALS among several neurodegenerative diseases [14\*], and to be specific to sporadic disease, as GluR2 mRNA was fully edited in G93A and H46R SOD1 transgenic rat models of familial ALS, and in humans with spinal and bulbar muscular atrophy (SBMA) [33\*] (Figure 2).

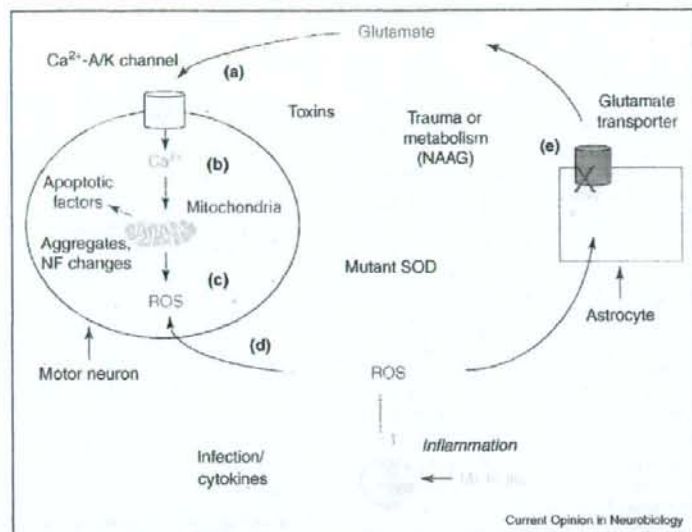
Figure 2



$\text{Ca}^{2+}$  or  $\text{Zn}^{2+}$  influx through AMPA receptors is regulated by the GluR2 subunit. AMPA receptors with GluR2 that has been edited at the Q/R site are  $\text{Ca}^{2+}$ -impermeable, but those lacking GluR2 entirely or with unedited GluR2 are  $\text{Ca}^{2+}$ -permeable. Under basal conditions, hippocampal pyramidal neurons (HPNs) have relatively few  $\text{Ca}^{2+}$  permeable AMPA channels comprising AMPA receptors lacking GluR2, whereas motor neurons (MNs) possess a substantial number of these channels. After ischemia, a decrease in GluR2 mRNA expression in CA1 hippocampal pyramidal neurons results in increased numbers of  $\text{Ca}^{2+}$  permeable AMPA channels lacking GluR2, contributing to their delayed degeneration (Of note, a recent study suggests that loss of editing efficiency might also contribute to increased  $\text{Ca}^{2+}$  permeable AMPA channel expression after ischemia; see update). By contrast, MNs in sporadic ALS express considerable unedited GluR2 mRNA, probably resulting in an increased number of  $\text{Ca}^{2+}$  permeable AMPA channels containing unedited GluR2. In either case, an increase in the proportion of  $\text{Ca}^{2+}$  permeable AMPA channels enables increased  $\text{Ca}^{2+}$  and/or  $\text{Zn}^{2+}$  entry into the cytoplasm, which contributes to neuronal death partly through effects on mitochondria. Red, orange and white cylinders represent edited GluR2, unedited GluR2 and AMPA receptor subunits other than GluR2 (GluR1, 3 or 4), respectively.

Many recent studies support the theory that  $\text{Ca}^{2+}$  permeable AMPA channels have a crucial role in MN degeneration in diverse conditions. A recent study found ventral root avulsion (see glossary) to cause selective decreases in the GluR2 protein [34], probably contributing to the MN injury in that condition. A  $\text{Ca}^{2+}$  permeable AMPA channel blocker was found to be protective in a model of virus-induced MN degeneration [35\*]. Transgenic animal studies have recently solidified the link between  $\text{Ca}^{2+}$  permeable AMPA channels and MN loss in SOD1-linked familial forms of ALS. Specifically, mice with modified GluR2 (GluR2-N), which results in production of AMPA channels with enhanced  $\text{Ca}^{2+}$  permeability, had late life MN degeneration [36\*\*], and crossing either these mice or mice lacking GluR2 entirely with mice with the G93A

Figure 3



A feed-forward model of ALS pathogenesis. Present observations provide the basis for a feed-forward cycle leading to selective MN injury in ALS. (a) Elevations of extracellular glutamate induce (b) excessive  $\text{Ca}^{2+}$  entry into MNs (through  $\text{Ca}^{2+}$  permeable AMPA channels), where it is taken up by mitochondria, (c) with consequent ROS generation and, possibly, activation of apoptotic pathways, either of which would injure the neuron. (d) The ROS could pass across the MN plasma membrane and (e) disrupt astrocytic glutamate transporters, thereby causing further rises in extracellular glutamate. Such a cycle could, in principle, be triggered at different sites (e.g., via glutamate rises or oxidative stress), and thus might be compatible with a multiplicity of inciting mechanisms (suggested in dashed boxes) leading into a common self-propagating disease pathway. Reprinted from [42] with permission from Elsevier.

SOD1 model of ALS resulted in marked acceleration of the disease [37]. Conversely, when mice with a decreased number of  $\text{Ca}^{2+}$  permeable AMPA channels in their MNs (via targeted GluR2 overexpression) were crossed with the G93A mice, the disease was significantly delayed [38].

Mechanisms through which the presence of  $\text{Ca}^{2+}$  permeable AMPA channels contributes to excitotoxic MN injury are being elucidated. Although these channels enable rapid  $\text{Ca}^{2+}$  entry, MNs buffer cytosolic  $\text{Ca}^{2+}$  loads poorly [39], and consequently much of the  $\text{Ca}^{2+}$  is readily taken up into mitochondria, resulting in strong ROS generation [40,41]. Furthermore, *in vitro* studies indicated that ROS produced in MNs in response to  $\text{Ca}^{2+}$  permeable AMPA channel activation might induce oxidative dysfunction of glutamate transporters in surrounding astrocytes [42]. This mechanism could play a role in the glutamate transport disruption seen in ALS, and provides the basis for a feed-forward cycle that could be integral to progression of the disease [42] (Figure 3).

### Role in ischemia

After transient global ischemia, HPNs, particularly in the CA1 subzone of the hippocampus, conspicuously

degenerate, often with a delay of several days. Under basal conditions, HPNs have few  $\text{Ca}^{2+}$  permeable AMPA channels. However, recent studies suggest that limited numbers of these channels are present, and they appear to be mainly localized to dendritic branches remote from the soma, where they are difficult to detect electrophysiologically [43–45].

Observations that GluR2 mRNA is markedly and selectively downregulated in CA1 HPNs after ischemia have led to an hypothesis that consequent increases in the number of  $\text{Ca}^{2+}$  permeable AMPA channels contribute to the delayed neurodegeneration [12] (Figure 2). Studies in recent years have provided considerable support to this hypothesis. First, GluR2 protein levels are decreased and AMPA-mediated  $\text{Ca}^{2+}$  currents are increased after ischemia [11]. Also, increasing the number of  $\text{Ca}^{2+}$  permeable AMPA channels in CA1 resulted in an increased vulnerability of HPNs to ischemic injury [46], whereas elevating GluR2 levels appeared to be protective [47]. Finally, some neuroprotection was observed upon addition of a  $\text{Ca}^{2+}$  permeable AMPA channel blocker many hours to days after the induction of ischemia [48]. This suggests that new treatments targeting these channels could



provide therapeutic benefits in humans even when given well after the ischemic episode.

Intriguingly, recent studies suggest that  $Zn^{2+}$  has multiple roles in this delayed selective neurodegeneration. In an *in vitro* slice model of acute ischemia, addition of either an extracellular  $Zn^{2+}$  chelator or a  $Ca^{2+}$  permeable AMPA channel blocker decreased both  $Zn^{2+}$  accumulation and consequent neuronal injury [21]. In an *in vivo* animal model, addition of an extracellular  $Zn^{2+}$  chelator either before or several days (but not several hours) after ischemia afforded neuroprotection. The early application of the chelator attenuated the downregulation of GluR2, suggesting a role for  $Zn^{2+}$  in signaling the increase in  $Ca^{2+}$  permeable AMPA channels. Whereas, late application of chelator, after  $Ca^{2+}$  permeable AMPA channel numbers had already risen, attenuated the late rise in intracellular  $Zn^{2+}$  associated with injury, suggesting that  $Ca^{2+}$  permeable AMPA channel dependent intracellular  $Zn^{2+}$  accumulation contributes to the delayed injury [49\*].

## Conclusions

Recent findings, reviewed above, suggest that increasing the number of  $Ca^{2+}$  permeable AMPA channels might contribute crucially to neurodegeneration in sporadic ALS and ischemia. The increase in  $Ca^{2+}$  permeable AMPA channels in these conditions could be achieved through different mechanisms: deficiencies in GluR2 mRNA editing in sporadic ALS or decreased levels of GluR2 mRNA in ischemia (Figure 2). In addition, basal levels of  $Ca^{2+}$  permeable AMPA channels appear to contribute to familial ALS associated with SOD1 mutations.  $Ca^{2+}$  permeable AMPA channels are probably also involved in other conditions including epilepsy and Alzheimer's disease, in which decreases in levels of GluR2 have been reported.

There are presently no selective  $Ca^{2+}$  permeable AMPA channel antagonists available for human trials or even for systemic administration in animals. Yet, the fact that  $Ca^{2+}$  permeable AMPA channels only constitute a minority of AMPA channels on most neurons makes them particularly attractive targets for therapeutics, as it could be possible to block much of the current through these channels without causing the degree of functional impairment that would accompany a comparable level of NMDA or total AMPA channel blockade. Furthermore, because an increase in  $Ca^{2+}$  permeable AMPA channel number might be integral to their pathological roles in certain conditions, in addition to the development of pharmacological antagonists, strategies for reducing their numbers or preventing their upregulation might also provide useful avenues for therapy.

## Update

In a recent study [51\*\*], Peng *et al.* report that forebrain ischemia in adult rats selectively disrupts Q/R site

editing and the expression of GluR2 subunit mRNA in vulnerable neurons. The authors provide further evidence that the editing defect contributes to the consequent neurodegeneration of CA1 HPNs. Thus, these data suggest that alterations of GluR2 editing might not be unique to ALS, and that this mechanism might also contribute to delayed neurodegeneration after transient ischemia.

## Acknowledgements

This work was supported by National Institutes of Health grant NS36548 (JH Weiss), a grant from the Muscular Dystrophy Association (JH Weiss), and a grant-in-aid for Scientific Research on Priority Areas from the Ministry of Education, Culture, Sports, Science and Technology of Japan 14017020, 15016030, 16015228 (S Kwak).

## References and recommended reading

Papers of particular interest, published within the annual period of review, have been highlighted as:

- of special interest
  - of outstanding interest
1. Seeburg PH, Single F, Kuner T, Higuchi M, Sprengel R: Genetic manipulation of key determinants of ion flow in glutamate receptor channels in the mouse. *Brain Res* 2001, 907:233-243.
  2. Kawahara Y, Kwak S: Excitotoxicity and ALS, what is unique about the AMPA receptors expressed on spinal motor neurons? *Amyotroph Lateral Scler Other Motor Neuron Disord* 2005, 6:131-144.
  3. Liu SQ, Cull-Candy SG: Synaptic activity at calcium-permeable AMPA receptors induces a switch in receptor subtype. *Nature* 2000, 405:454-458.
  4. Gardner SM, Takamiya K, Xia J, Suh JG, Johnson R, Yu S, Hagan RL: Calcium-permeable AMPA receptor plasticity is mediated by subunit-specific interactions with PICK1 and NSF. *Neuron* 2005, 45:903-915.
  5. Liu SJ, Cull-Candy SG: Subunit interaction with PICK and GRIP controls  $Ca^{2+}$  permeability of AMPARs at cerebellar synapses. *Nat Neurosci* 2005, 8:768-775.
  6. Greger IH, Khatri L, Kong X, Ziff EB: AMPA receptor tetramerization is mediated by Q/R editing. *Neuron* 2003, 40:763-774.
  7. Greger IH, Khatri L, Ziff EB: RNA editing at arg607 controls AMPA receptor exit from the endoplasmic reticulum. *Neuron* 2002, 34:759-772.
  8. Beattie EC, Stellwagen D, Morishita W, Bresnahan JC, Ha BK, Von Zastrow M, Beattie MS, Malenka RC: Control of synaptic strength by glial TNF $\alpha$ . *Science* 2002, 295:2282-2285.
  9. Ogoshi F, Yin HZ, Kuppambatti Y, Song B, Amindari S, Weiss JH: Tumor necrosis factor- $\alpha$  (TNF- $\alpha$ ) induces rapid insertion of  $Ca^{2+}$ -permeable alpha-amino-3-hydroxy-5-methyl-4-isoxazole-propionate (AMPA)/kainate (CA-A/K) channels in a subset of hippocampal pyramidal neurons. *Exp Neurol* 2005, 193:384-393.
  10. The authors use  $Ca^{2+}$  imaging techniques to demonstrate membrane insertion of  $Ca^{2+}$  permeable AMPA channel in subpopulations of hippocampal pyramidal neurons in response to exposure to the soluble cytokine, TNF- $\alpha$ .



10. Stellwagen D, Beattie EC, Seo JY, Malenka RC: **Differential regulation of AMPA receptor and GABA receptor trafficking by tumor necrosis factor- $\alpha$** . *J Neurosci* 2005, **25**:3219-3228.  
The authors report that TNF- $\alpha$  induces preferential exocytosis of GluR2-lacking AMPA receptors in hippocampal neurons.
11. Gorter JA, Petrozzino JJ, Aronica EM, Rosenbaum DM, Opitz T, Bennett MV, Connor JA, Zukin RS: **Global ischemia induces downregulation of GluR2 mRNA and increases AMPA receptor-mediated  $Ca^{2+}$  influx in hippocampal CA1 neurons of gerbil**. *J Neurosci* 1997, **17**:6179-6188.
12. Pellegrini-Giamperio DE, Gorter JA, Bennett MV, Zukin RS: **The GluR2 (GluR-B) hypothesis:  $Ca^{2+}$ -permeable AMPA receptors in neurological disorders**. *Trends Neurosci* 1997, **20**:464-470.
13. Kawahara Y, Ito K, Sun H, Aizawa H, Kanazawa I, Kwak S: **Glutamate receptors: RNA editing and death of motor neurons**. *Nature* 2004, **427**:801.  
The authors demonstrate that in sporadic ALS, MNs, but not Purkinje cells, have abundant GluR2 mRNA that is unedited at the Q/R site. The specificity of this finding to MNs and the demonstrated ability of the activation of  $Ca^{2+}$  permeable AMPA channels to injure neurons suggest that this molecular change might be tightly linked to the etiology of MN death in sporadic ALS.
14. Kwak S, Kawahara Y: **Deficient RNA editing of GluR2 and neuronal death in amyotrophic lateral sclerosis**. *J Mol Med* 2005, **83**:110-120.  
The authors review the AMPA receptor-mediated neuronal death in ALS, and discuss mechanisms that might underlie the underediting of GluR2 mRNA in MNs.
15. Takuma H, Kwak S, Yoshizawa T, Kanazawa I: **Reduction of GluR2 RNA editing, a molecular change that increases calcium influx through AMPA receptors, selective in the spinal ventral gray of patients with amyotrophic lateral sclerosis**. *Ann Neurol* 1999, **46**:806-815.
16. Hong SJ, Dawson TM, Dawson VL: **Nuclear and mitochondrial conversations in cell death: PARP-1 and AIF signaling**. *Trends Pharmacol Sci* 2004, **25**:259-264.
17. Koh JY, Suh SW, Gwag BJ, He YY, Hsu CY, Choi DW: **The role of zinc in selective neuronal death after transient global cerebral ischemia**. *Science* 1996, **272**:1013-1016.
18. Lee JY, Kim JH, Palmiter RD, Koh JY: **Zinc released from metallothionein-III may contribute to hippocampal CA1 and thalamic neuronal death following acute brain injury**. *Exp Neurol* 2003, **184**:337-347.
19. Jia Y, Jeng JM, Sensi SL, Weiss JH:  **$Zn^{2+}$  currents are mediated by calcium-permeable AMPA/kainate channels in cultured murine hippocampal neurons**. *J Physiol* 2002, **543**:35-48.
20. Sensi SL, Yin HZ, Carriedo SG, Rao SS, Weiss JH: **Preferential  $Zn^{2+}$  influx through  $Ca^{2+}$ -permeable AMPA/kainate channels triggers prolonged mitochondrial superoxide production**. *Proc Natl Acad Sci USA* 1999, **96**:2414-2419.
21. Yin HZ, Sensi SL, Ogoshi F, Weiss JH: **Blockade of  $Ca^{2+}$ -permeable AMPA/kainate channels decreases oxygen-glucose deprivation-induced  $Zn^{2+}$  accumulation and neuronal loss in hippocampal pyramidal neurons**. *J Neurosci* 2002, **22**:1273-1279.
22. Kim YH, Koh JY: **The role of NADPH oxidase and neuronal nitric oxide synthase in zinc-induced poly(ADP-ribose) polymerase activation and cell death in cortical culture**. *Exp Neurol* 2002, **177**:407-418.
23. Jiang D, Sullivan PG, Sensi SL, Steward O, Weiss JH:  **$Zn^{2+}$  induces permeability transition pore opening and release of pro-apoptotic peptides from neuronal mitochondria**. *J Biol Chem* 2001, **276**:47524-47529.
24. Sensi SL, Ton-That D, Sullivan PG, Jonas EA, Gee KR, Kaczmarek LK, Weiss JH: **Modulation of mitochondrial function by endogenous  $Zn^{2+}$  pools**. *Proc Natl Acad Sci USA* 2003, **100**:6157-6162.
25. Bossy-Wetzell E, Talantova MV, Lee WD, Schotzke MN, Harrop A, Mathews E, Gotz T, Han J, Ellisman MH, Perkins GA et al.: **Crosstalk between nitric oxide and zinc pathways to neuronal cell death involving mitochondrial dysfunction and p38-activated  $K^{+}$  channels**. *Neuron* 2004, **41**:351-365.
26. Rothstein JD, Martin LJ, Kuncl RW: **Decreased glutamate transporter by the brain and spinal cord in amyotrophic lateral sclerosis**. *N Engl J Med* 1992, **326**:1464-1468.
27. Carriedo SG, Yin HZ, Weiss JH: **Motor neurons are selectively vulnerable to AMPA/kainate receptor-mediated injury in vitro**. *J Neurosci* 1996, **16**:4069-4079.
28. Rothstein JD, Jin L, Dykes-Hoberg M, Kuncl RW: **Chronic inhibition of glutamate uptake produces a model of slow neurotoxicity**. *Proc Natl Acad Sci USA* 1993, **90**:6591-6595.
29. Van Den Bosch L, Vandenberghe W, Klaassen H, Van Houtte E, Robberecht W:  **$Ca^{2+}$ -permeable AMPA receptors and selective vulnerability of motor neurons**. *J Neural Sci* 2000, **180**:29-34.
30. Vandenberghe W, Robberecht W, Brorson JR: **AMPA receptor calcium permeability, GluR2 expression, and selective motoneuron vulnerability**. *J Neurosci* 2000, **20**:123-132.
31. Kawahara Y, Kwak S, Sun H, Ito K, Hashida H, Aizawa H, Jeong S-Y, Kanazawa I: **Human spinal motoneurons express low relative abundance of GluR2 mRNA: An implication for excitotoxicity in ALS**. *J Neurochem* 2003, **85**:680-689.
32. Sun H, Kawahara Y, Ito K, Kanazawa I, Kwak S: **Expression profile of AMPA receptor subunit mRNA in single adult rat brain and spinal cord neurons in situ**. *Neurosci Res* 2005, **52**:228-234.
33. Kawahara Y, Sun H, Ito K, Hideyama T, Aoki M, Sobue G, Tsuji S, Kwak S: **Underediting of GluR2 mRNA, a neuronal death inducing molecular change in sporadic ALS, does not occur in motor neurons in ALS1 or SBMA**. *Neurosci Res* 2006, **54**:11-14.  
Although animals carrying mutated human SOD1 are the most widely used models for ALS, this paper reports that in these animals, and in humans with SBMA, the GluR2 editing defects do not occur. This suggests that differing molecular mechanisms underlie sporadic and familial forms of ALS.
34. Nagano I, Murakami T, Shioe M, Abe K, Itoyama Y: **Ventral root avulsion leads to downregulation of GluR2 subunit in spinal motoneurons in adult rats**. *Neuroscience* 2003, **117**:139-146.
35. Darman J, Backovic S, Dike S, Maragakis NJ, Krishnan C, Rothstein JD, Irani DN, Kerr DA: **Viral-induced spinal motor neuron death is non-cell-autonomous and involves glutamate excitotoxicity**. *J Neurosci* 2004, **24**:7566-7575.  
The authors report that  $Ca^{2+}$  permeable AMPA channel blockers offer protection against MN death caused by a viral infection, supporting the contention that  $Ca^{2+}$  permeable AMPA channel activation contributes to MN degeneration in diverse conditions.
36. Kuner R, Groom AJ, Bresink I, Komau HC, Stefovskaya V, Muller G, Hartmann B, Tschauner K, Waibel S, Ludolph AC et al.: **Late-onset motoneuron disease caused by a functionally modified AMPA receptor subunit**. *Proc Natl Acad Sci USA* 2005, **102**:5826-5831.  
In this study, mice transgenic for GluR-B(N), an artificial gene resulting in increased  $Ca^{2+}$  permeability of AMPA channels, developed slow onset of MN loss, indicating that increasing  $Ca^{2+}$  permeable AMPA channel numbers (as probably occurs from underediting of GluR2) does result in preferential MN injury. Additional presence of mutant SOD1 in these animals accelerated disease progression, indicating synergism between  $Ca^{2+}$  permeable AMPA channel activation and mutant SOD1 in mediating MN degeneration.
37. Van Damme P, Braeken D, Callewaert G, Robberecht W, Van Den Bosch L: **GluR2 deficiency accelerates motor neuron degeneration in a mouse model of amyotrophic lateral sclerosis**. *J Neuropathol Exp Neurol* 2005, **64**:605-612.  
The authors report that deletion of the GluR2 subunit caused increased  $Ca^{2+}$  permeable AMPA channel number in MNs and accelerated MN loss in SOD1 mutant mice, again indicating synergistic effects of  $Ca^{2+}$  permeable AMPA channel activation and mutant SOD1.
38. Tateno M, Sadakata H, Tanaka M, Itohara S, Shin RM, Miura M, Masuda M, Acsaki T, Urushitani M, Misawa H et al.: **Calcium-permeable AMPA receptors promote misfolding of mutant SOD1 protein and development of amyotrophic lateral**



- sclerosis in a transgenic mouse model. *Hum Mol Genet* 2004, 13:2183-2196.
- Taking the opposite approach to the two papers above [36\*\*, 37\*], these authors find that decreasing the number of  $Ca^{2+}$ -permeable AMPA channels in MNs (by targeted GluR2 overexpression) delays the MN loss and prolongs survival in SOD1 mutant mice. This provides further evidence for a role of  $Ca^{2+}$ -permeable AMPA channel activation in this familial form of ALS.
39. Lips MB, Keller BU: **Endogenous calcium buffering in motoneurons of the nucleus hypoglossus from mouse.** *J Physiol* 1998, 511:105-117.
  40. Carriedo SG, Sensi SL, Yin HZ, Weiss JH: **AMPA exposures induce mitochondrial  $Ca^{2+}$  overload and ROS generation in spinal motor neurons in vitro.** *J Neurosci* 2000, 20:240-250.
  41. Rao SD, Yin HZ, Weiss JH: **Disruption of glial glutamate transport by reactive oxygen species produced in motor neurons.** *J Neurosci* 2003, 23:2627-2633.
  42. Rao SD, Weiss JH: **Excitotoxic and oxidative cross-talk between motor neurons and glia in ALS pathogenesis.** *Trends Neurosci* 2004, 27:17-23.  
The authors consider the evidence that ROS produced in MNs might account for disruption of astrocytic glutamate transport, and discuss how this mechanism could underlie a feed-forward model of ALS progression and provide a basis for observations that MN loss in ALS is "non-cell-autonomous".
  43. Lerma J, Morales M, Ibarz JM, Somohano F: **Rectification properties and  $Ca^{2+}$  permeability of glutamate receptor channels in hippocampal cells.** *Eur J Neurosci* 1994, 6:1080-1088.
  44. Ogoshi F, Weiss JH: **Heterogeneity of  $Ca^{2+}$ -permeable AMPA/kainate channel expression in hippocampal pyramidal neurons: fluorescence imaging and immunocytochemical assessment.** *J Neurosci* 2003, 23:10521-10530.
  45. Yin HZ, Sensi SL, Carriedo SG, Weiss JH: **Dendritic localization of  $Ca^{2+}$ -permeable AMPA/kainate channels in hippocampal pyramidal neurons.** *J Comp Neurol* 1999, 409:250-260.
  46. Anzai T, Tsuzuki K, Yamada N, Hayashi T, Iwakuma M, Inada K, Kameyama K, Hoka S, Saji M: **Overexpression of  $Ca^{2+}$ -permeable AMPA receptor promotes delayed cell death of hippocampal CA1 neurons following transient forebrain ischemia.** *Neurosci Res* 2003, 46:41-51.
  47. Liu S, Lau L, Wei J, Zhu D, Zou S, Sun HS, Fu Y, Liu F, Lu Y: **Expression of  $Ca^{2+}$ -permeable AMPA receptor channels primes cell death in transient forebrain ischemia.** *Neuron* 2004, 43:43-55.  
These authors varied  $Ca^{2+}$ -permeable AMPA channel levels in both directions, and found that decreasing their number (by overexpression of edited GluR2) attenuated ischemic injury in the CA1 subfield, whereas increasing  $Ca^{2+}$ -permeable AMPA channels (by overexpression of unedited GluR2) resulted in new ischemic damage to granule neurons.
  48. Noh KM, Yokota H, Mashiko T, Castillo PE, Zukin RS, Bennett MV: **Blockade of calcium-permeable AMPA receptors protects hippocampal neurons against global ischemia-induced death.** *Proc Natl Acad Sci USA* 2005, 102:12230-12235.  
The authors provide electrophysiological evidence for a substantial rise in the number of  $Ca^{2+}$ -permeable AMPA channels on CA1 pyramidal neurons at 42 h after transient global ischemia. In addition, they find that addition of a  $Ca^{2+}$ -permeable AMPA channel blocker between 9 and 40 h after the ischemia was partially protective and markedly reduced the rise in  $Zn^{2+}$  levels observed to precede neuronal death.
  49. Calderone A, Jover T, Mashiko T, Noh KM, Tanaka H, Bennett MV, Zukin RS: **Late calcium EDTA rescues hippocampal CA1 neurons from global ischemia-induced death.** *J Neurosci* 2004, 24:9903-9913.  
These authors report that addition of the  $Zn^{2+}$  chelator, Ca-EDTA, can decrease CA1 neuronal degeneration in distinct ways depending upon the time of delivery. Early Ca-EDTA (before ischemia) prevented the GluR2 downregulation, cytochrome C release and other indices of mitochondrial disruption. By contrast, late Ca-EDTA (48-60 h after ischemia), when GluR2 is already downregulated, attenuated the late  $Zn^{2+}$  rises observed to precede cell death. The findings of this and the previous paper [48\*\*] support the therapeutic efficacy of  $Ca^{2+}$ -permeable AMPA channel blockade or  $Zn^{2+}$  chelation when delivered long after an ischemic insult.
  50. Nishimoto Y, Hideyama T, Kawahar Y, Kwak S: **Reduction of RNA editing of an AMPA receptor subunit GluR2 and death of motor neurons in ALS (in Japanese).** *Clinical Neuroscience* 2006, 24:222-225.
  51. Peng PL, Zhong X, Tu W, Soundarapandian MM, Molner P, Zhu D, Lau L, Liu S, Liu F, Lu Y: **ADAR2-dependent RNA editing of AMPA receptor subunit GluR2 determines vulnerability of neurons in forebrain ischemia.** *Neuron* 2006, 49:719-733.  
The authors use single cell PCR to show that forebrain ischemia in adult rats selectively disrupts Q/R site editing through downregulation of the editing enzyme adar2. They also provide evidence that this editing defect contributes to the delayed selective degeneration of CA1 hippocampal pyramidal neurons.

# Aging of Complex Heart Rate Dynamics

Zbigniew R. Struzik, Junichiro Hayano, Rika Soma, Shin Kwak, and Yoshiharu Yamamoto

**Abstract**—We reveal unexpected origins of age induced departure from  $1/f$ -type temporal scaling in healthy human heart rate. Contrary to the widely established view, we provide evidence that age induced dynamical imbalance in the autonomic control is not due to the emergent functional dominance of the sympathetic nervous system (SNS), but due to emerging (age dependent) relative dynamic dominance of the parasympathetic nervous system function. In particular, we demonstrate that the age induced alterations of healthy heart rate dynamics asymptotically resemble those in so-called primary autonomic failure with neurogenic SNS dysfunction and in other neurodegenerative disorders, including Parkinson's disease even without known autonomic abnormalities. Based upon this, we propose a novel picture of "autonomic aging," characterized by an insufficiency of the SNS function to cope dynamically with various environmental stimuli.

**Index Terms**—Aging, autonomic nervous system, heart rate variability, multifractals,  $1/f$  noise.

## I. INTRODUCTION

HEALTHY human heart rate has been known to display fairly complex dynamics, exhibiting long-range temporal correlations [1], [2], non-Gaussianity of the increment's probability density function [1], as well as multifractality [3], [4], all reminiscent of real-world complex signals in physics, e.g., fluid turbulence [5], [6] and critical phenomena [7]–[9]. Physiologically, the origin of the complex dynamics of heart rate has been attributed to an intricate balance between the two branches of the autonomic nervous system: the parasympathetic (PNS) and the sympathetic (SNS) nervous systems, respectively, decreasing and increasing heart rate [1], [2], [4], [10]. In fact, Struzik *et al.* [11] recently reported that the disease-induced relative dysfunction of either PNS or SNS results in more correlated heart rate dynamics, but only the PNS dysfunction leads to reduced multifractality.

Although it has been conjectured that there is both a functional and a structural loss of complexity due to aging [12], the effect of aging on complex heart rate dynamics in humans has not been fully elucidated. Heart rate responses to selective and/or combined autonomic blockades of PNS and SNS [13],

[14], plasma concentration of the sympathetic neurotransmitters [15], and the magnitude of respiratory modulation of heart rate [16]–[19], one of the robust indicators of PNS function [20], [21], all exhibit changes compatible with the increased SNS and decreased PNS function with aging. This might lead to the conjecture that aging is associated with increased long-range correlation, as demonstrated previously [22]–[24], and with decreased multifractality, as have been observed in congestive heart failure (CHF) [3] with relative SNS augmentation [25], [26] and PNS dysfunction [25], [27].

Here, however, we present an unexpected observation regarding the complex dynamical interaction between two branches of the autonomic control system, namely that normative aging is associated with increased long-range correlation but with preserved multifractality. The direction of change is consistent with that observed in patients suffering from central SNS dysfunction due to primary autonomic failure (PAF) [28], [29], not with the direction observed in CHF. We believe that our findings will give rise to a novel picture of "autonomic aging" as a progressive loss of the SNS function and its ability to cope dynamically with various environmental stimuli.

## II. DATA

We analyze 115 healthy subjects (26 women and 89 men; ages 16–84 years) without any known disease affecting autonomic control of heart rate. They underwent ambulatory monitoring during normal daily life, and the long-term heart rate data were measured as sequential heart interbeat intervals. The total number of whole-day data sets is 181, as most of the subjects were examined for two consecutive days, with each data set containing on average  $10^5$  heartbeats. For each subject, on an individual basis, we have excluded the possibility of any bias in the results caused by two consecutive days of heart rate recording ( $p = 0.54$  by paired t-test for the individual daily Hurst exponent).

Details of the recruitment of the subjects, screening for medical problems, protocols and the data collection and preprocessing are described in [30]. We analyzed both whole-day data containing periods of sleep and waking and daytime data, with essentially identical results. In this paper, we present only daytime results.

As a reference, we describe the results previously obtained for 24-hour ambulatory heart rate dynamics of 10 PAF patients (3 women and 7 men) aged 54–77 years (mean age 64.8) [28], containing on average  $10^5$  heartbeats [11]. The selection of the subjects and the collection procedures for this data are described in [11]. PAF is clinically characterized as autonomic dysfunction, including orthostatic hypotension, impotence, bladder and bowel dysfunction and sweating defects, which primarily result from progressive neuronal degeneration of unknown cause. The main pathological finding related to autonomic dysfunction in PAF is severe loss of preganglionic and/or postganglionic sympathetic

Manuscript received October 20, 2004; revised May 8, 2005. This work was supported in part by the Japan Science and Technology Agency. Asterisk indicates corresponding author.

\*Z. R. Struzik is with the Educational Physiology Laboratory, Graduate School of Education, The University of Tokyo, 7-3-1 Hongo, Bunkyo-ku, Tokyo 113-0033, and PRESTO, Japan Science and Technology Agency, Kawaguchi, Saitama 332-0012, Japan (e-mail: Zbigniew.Struzik@p.u-tokyo.ac.jp).

J. Hayano is with the Core Laboratory, Nagoya City University Graduate School of Medical Sciences, Nagoya 467-8601, Japan.

R. Soma and Y. Yamamoto are with the Educational Physiology Laboratory, Graduate School of Education, The University of Tokyo, Tokyo 113-0033, Japan, and PRESTO, Japan Science and Technology Agency, Kawaguchi, Saitama 332-0012, Japan.

S. Kwak is with the Department of Neurology, Graduate School of Medicine, The University of Tokyo, Tokyo 113-0033, Japan.

Digital Object Identifier 10.1109/TBME.2005.859801



neurons [29], and it is, thus, considered that this group serves as an example of relative and neurogenic SNS dysfunction.

Further, we also include the results for 12 CHF subjects (3 women and 9 men, with ages between 22 and 71, average 60.8 years) [11]. For details of the data acquisition and pre-processing see [3].

Finally, in a combined group with PAF patients, we also use additional 24-hour ambulatory heart rate data obtained from 5 patients, including four Parkinson's disease (PD) patients and one patient (74 years, male) showing "pure akinesia," one of the clinical features of Parkinsonism, without known autonomic abnormalities, containing on average  $10^5$  heartbeats. All the PD patients had bradykinesia and rigidity-predominant PD with apparent L-dopa responsiveness. There were 4 men and 1 woman, with a mean age of 67.2 years (range 56 to 74 years) and the mean disease duration was 11.2 years (range 3 to 24 years). All the patients received regular antiparkinsonian medication before and during the test days. The data, 24-hour heartbeat intervals of the PD patients during a hospital stay, were collected using a portable ambulatory monitor [31].

### III. ANALYSIS METHODS

#### A. DFA Analysis of Aging

To evaluate the degree of long-range temporal correlation, the scaling exponent (the Hurst exponent  $H$ ) has been calculated by using (first-order) detrended fluctuation analysis (DFA) [32], [33], as described below.

We have (arbitrarily) selected a number of age groups to assess mean scaling per group. The groups chosen are less than forty (40-), forty to sixty (40-60), sixty to eighty (60-80), and above eighty (80+) years. We have analyzed the scaling behavior of the mean quantity (group mean)  $\bar{M}_{DFA}(s) = L^{-1} \sum_{l=1}^L \log_{10}(D_{DFA}^{(l)}(s))$ , where  $l$  indexes time series in the group. For each scale/resolution  $s$  as measured by the DFA window size, and for each integrated, normalized heartbeat interval time series  $\{F_i^{(l)} = T_l^{-1} \sum_{j=1}^i f_j^{(l)}\}_{(i=1, \dots, N_l), (l=1, \dots, L)}$ ,  $D_{DFA}^{(l)}(s)$  (total scalewise detrended fluctuation) has been calculated

$$D_{DFA}^{(l)}(s) = s^{-1} \sqrt{\frac{1}{K^{(l)}(s)} \sum_{k=1}^{K^{(l)}(s)} (F_k^{(l)} - P_k(s))^2}$$

$P_k(s)$  denotes the local least-squares linear fit in each DFA window  $k$ , and  $K^{(l)}(s)$  is the number of windows per scale  $s$ . Integration of the input heartbeat intervals is performed according to standard DFA practice, and the norm used is the elapsed time  $T_l = \sum_{i=1}^{N_l} f_i^{(l)}$ . The normalization applied allows us to compute group averages of records of different duration, and to compare the mean absolute levels of variability per resolution  $s$ ; for each resolution  $s$ , the quantity  $\bar{M}_{DFA}(s)$  measures the (logarithmic) scalewise mean of the normalized DFA (the sum of the logarithm of detrended fluctuations for each group of time series at this resolution). The Hurst exponent was computed from the log-log fit to the group averaged DFA values over the selected range of scales (20-4000 beats).

#### B. Multifractal Analysis of Aging

We have also tested the multifractal properties of the data using the wavelet-based multifractal methodology [34]. We

apply the second derivative of the Gaussian to the data as the mother wavelet before calculating the partition function  $Z_q(s)$ , defined as the sum of the  $q$ th powers of the local maxima of the modulus of the wavelet transform coefficients at scale  $s$ . The power law scaling of  $Z_q(s)$  for  $13 < s < 850$  then yields the scaling exponents  $\tau(q)$  (the multifractal spectrum). The multifractal spectrum is related to the singularity spectrum  $D(h)$ , where  $D(h_0)$  is the fractal dimension of the subset of the original time series characterized by a local Hurst exponent  $h = h_0$  [35], through a Legendre transform  $D(h) = qh - \tau(q)$  with  $h = d\tau(q)/dq$ .

In order to provide group mean values, we have analyzed the scaling behavior of the mean quantity  $\bar{M}_{WTMM}(q, s) = L^{-1} \sum_{l=1}^L \log_{10}(Z_{WTMM}^{(l)}(q, s))$ , where  $l$  indexes time series in the group. For each scale/resolution  $s$  as measured by the wavelet size, and for each integrated, normalized heartbeat interval time series  $\{F_i^{(l)} = T_l^{-1} \sum_{j=1}^i f_j^{(l)}\}_{(i=1, \dots, N_l), (l=1, \dots, L)}$ ,  $Z_{WTMM}^{(l)}(q, s)$  (the multifractal partition function) has been calculated

$$Z_{WTMM}^{(l)}(q, s) = \sum_{k=1}^{K^{(l)}(s)} (WT_{\omega_k}(s)(F^{(l)}))^q$$

$WT_{\omega_k}(s)(F^{(l)})$  denotes the  $k$ th maximum of the modulus of the wavelet transform  $WT$  of the time series  $F^{(l)}$ , and  $K^{(l)}(s)$  is the number of maxima per scale  $s$ . As in the case of the DFA analysis above, the norm used is the elapsed time  $T_l = \sum_{i=1}^{N_l} f_i^{(l)}$ .

Similarly to the case of the mean DFA analysis, the normalization applied allows us to compute group averages of records of different duration; for each resolution  $s$ , the quantity  $\bar{M}_{WTMM}(s)$  measures the (logarithmic) scalewise mean of the normalized partition function  $Z(q, s)$  parameterized with the moment  $q$ .  $\tau(q)$  is, thus, obtained by linear fit to the mean quantity  $\bar{M}_{WTMM}(s)$  versus  $\log(s)$ . The Legendre transform is implemented by a linear fit in the  $\tau(q)$  domain; from 100 samples of  $q$  in the range  $-15 \leq q \leq 15$ , one-quarter, i.e., 25, of the available points is used to obtain  $h(q)$  as a function of  $q$ , as the best local linear fit to  $\tau(q)$ , centered at  $q$ .  $D(h(q))$  is then calculated in a straightforward way. Note that only the useful range  $-6 \leq q \leq 6$  is shown in the  $\tau(q)$  plots and used for  $D(h)$  plots.

### IV. RESULTS

In Fig. 1, we show the dependence of the estimated scaling exponent  $H$  for the range of resolutions used (16-4000 beats) on age for each healthy subject. A steady increase in  $H$  can be observed, consistent with previously reported findings using Fourier methods of scaling exponent estimation [19], [24] and DFA for age groups of young and old [22]-[24].

In Fig. 2, we show the scaling behavior of the  $\log_{10}(\bar{D}_{DFA}(s))$  versus  $\log_{10}(s)$  for the different age groups. We identify a systematic tendency of the decrease in scalewise variability with aging for the healthy group. This holds for the entire compared resolution range of 4-4000 beats as measured by the DFA window size  $s$ .

Although the extremely low PAF variability is not reached by healthy adults even in the group over the age of 80 years old, the levels of variability at the highest resolutions (and lowest



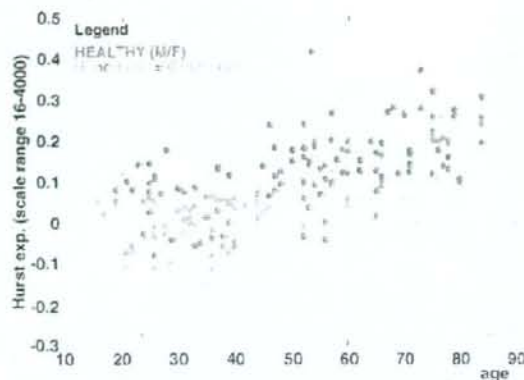


Fig. 1. Typical age-related departure from  $1/f$  scaling for healthy heart rate showing a steady increase. First-order DFA, i.e., linear trend removal [32], is used for the estimation of the Hurst exponent  $H$  from the daytime records of heartbeat intervals of healthy subjects.

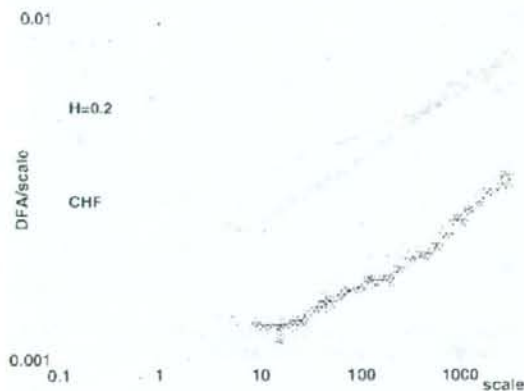


Fig. 2. Scale dependency of the mean detrended fluctuation  $\bar{D}_{DFA}(s)$  for four age groups of healthy subjects and for the PAF patients. Detrended fluctuations have been calculated with first-order DFA, i.e., linear trend removal [32]. The vertical bars represent the standard deviations of the group means.

beat numbers) remain relatively well conserved for all ages, reflecting the preservation of high-frequency fluctuations of heart rate, indicative of the intact PNS function [20], [21], in the elder groups as well as in the PAF patients. This contrasts with the reported [11] considerable decrease in CHF variability at all resolutions, including variability decrease the highest resolutions (presumably due to the decreased PNS function).

Consistent with the results depicted in Fig. 1, we confirm the age-related systematic (and substantial) increase in the Hurst exponent  $H$  of the analyzed age groups from  $1/f$  corresponding with  $H = 0.0$  to  $H > 0.2$  for advanced age, i.e., toward the value which is both observed in the relative PNS dysfunction by CHF and in the PAF induced relative SNS dysfunction [11] (Fig. 2). This effect has been observed for the entire range of resolutions with almost consistent scaling, which for all groups analyzed stretches from about 20 beats up to the maximum resolution used of 4000 beats (DFA window size).

From the above established facts, it would be difficult to determine which branch of the autonomic nervous system suffers

due to aging. Affecting the PSN/SNS balance by both the relative and neurogenic SNS dysfunction by PAF and by the relative PNS dysfunction by CHF results in a strong decrease in scale-wise variability and an increase of the scaling exponent  $H$ . The only indicator of the intact PNS function in the above is the relatively well-conserved variability at the highest resolutions, i.e., at the lowest beat numbers, as also suggested in a previous study [16].

Therefore, in order to provide further evidence for the preserved PNS function with aging, we have also tested the multifractal properties of the data, shown to be observed only with the functional PNS [11], using the wavelet-based multifractal methodology [34].

We obtain a comparable, wide singularity spectra  $D(h)$  for all the healthy age groups, indicative of preserved multifractality with advancing age (Fig. 3). While multifractality has been shown to be nearly lost in the case of CHF patients [3], it has recently been shown to be maintained in the case of PAF patients [11]. Thus, it seems that autonomic aging mimics PAF, but not CHF with the SNS predominance, and we have obtained surprising evidence that the age induced dynamical imbalance in the autonomic control may not reflect the relative increase in SNS function but rather be related to a dynamical and relative decrease of it.

## V. EMERGING PICTURE OF AUTONOMIC AGING

At present, the mechanism for this observation is unknown, but two possibilities exist. First, the elderly are known to show a decrease in vasoconstrictive responses to sympathetic stimulation [36], which would lead to functionally similar effects to PAF with neurogenic SNS dysfunction. Second, age-related degeneration in the brain stem dopaminergic, as well as noradrenergic neurons [37], and the resultant direct and/or indirect (through the limbic system) effects on the medullary cardiovascular centers may be responsible for the similarity in the heart rate dynamics of the elderly to those of PAF patients, and possibly of PD patients even without autonomic failure. Aging is indeed known to be associated with manifestations of signs of Parkinsonism [38], of which neuronal degeneration in the dopaminergic substantia nigra and the noradrenergic locus coeruleus is the main neuropathology [39].

To confirm the second possibility, we created a combined group of "simulated autonomic aging" by mixing the data from the PAF group with the heart rate data obtained from 5 patients, including four PD patients and one patient (74 years, male) showing "pure akinesia," one of the clinical features of Parkinsonism, without known autonomic abnormalities.

We verify that mixing PD patients without known autonomic abnormality with PAF patients also results in a consistent increase in the DFA slope greater than that of the oldest age group of over eighty years of age, see Fig. 4. As shown in Fig. 5, this new "simulated autonomic aging" group shows a systematic increase in the DFA slope, even when compared with the age-matched healthy controls, with preserved multi-fractality (Fig. 6). This suggests that these neurodegenerative diseases have a similar effect on heart rate dynamics, i.e., increased Hurst exponent and preserved multifractality, to that of normative aging. It is of note that both PAF [29] and PD [40] are known to have sympathetic dysfunction, consistent with a scenario



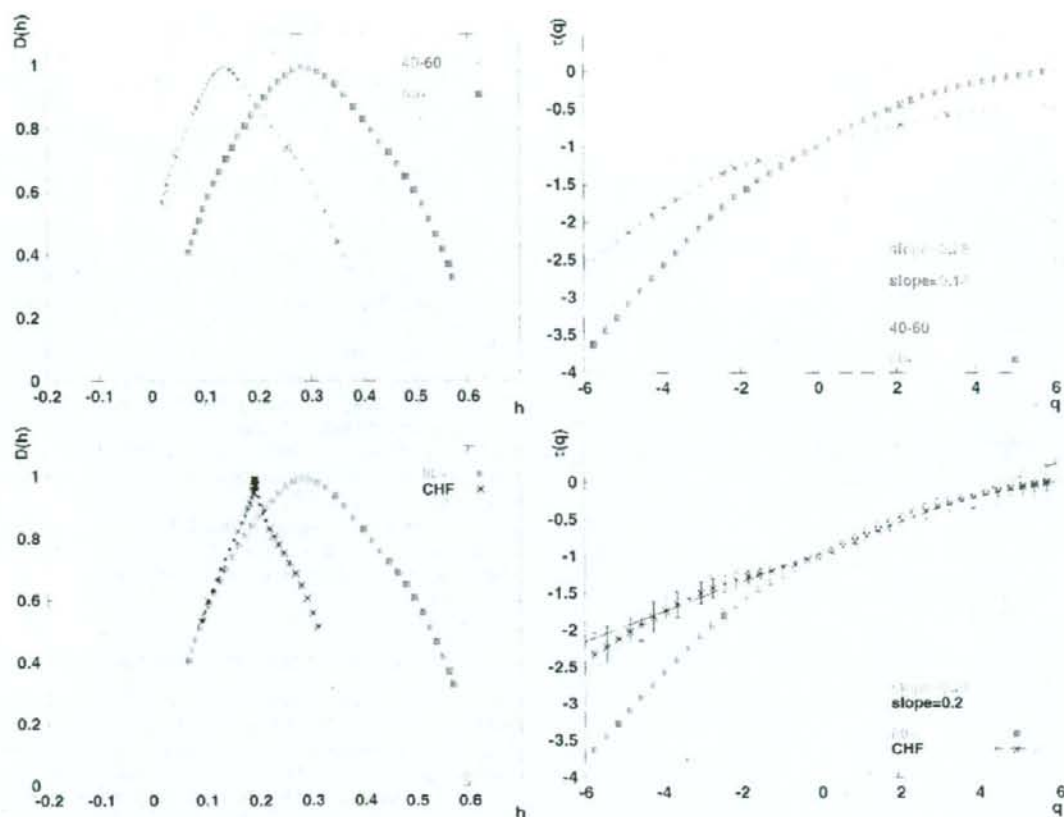


Fig. 3. Singularity spectra  $D(h)$ , together with the  $\tau(q)$  spectra of moments of the partition function  $Z_q(x)$ , for four age groups of healthy subjects and for PAF patients. For reference, CHF and PAF spectra are also outlined [11]. Note the preserved width of  $D(h)$ , even for subjects in the oldest age group.

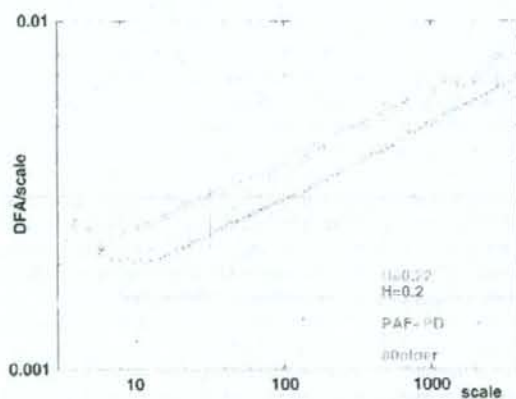


Fig. 4. Scale dependency of the mean detrended fluctuation  $\bar{D}_{TPA}(s)$  for the 80+ age group of healthy subjects and for both the PAF patients group and the "simulated autonomic aging" group (PAF + PD). Detrended fluctuations have been calculated with first-order DFA, i.e., linear trend removal [32]. The vertical bars represent the standard deviations of the group means.

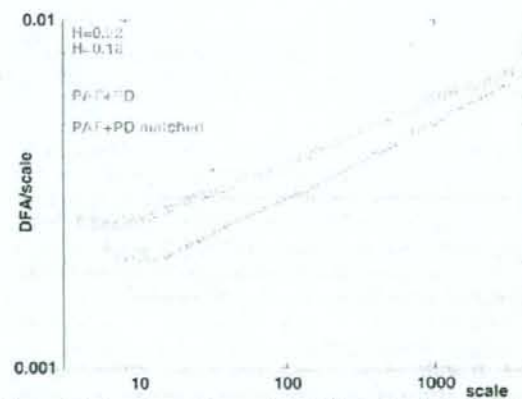


Fig. 5. Scale dependency of the mean detrended fluctuation  $\bar{D}_{TPA}(s)$  for both the PAF patients group and the "simulated autonomic aging" group (PAF + PD), compared with healthy subjects matched by age and gender with the patients in the two groups. Detrended fluctuations have been calculated with first-order DFA, i.e., linear trend removal [32]. The vertical bars represent the standard deviations of the group means.

of decreased SNS function as a manifestation of autonomic aging. It may be important to verify whether PD patients alone

display "autonomic aging" tendencies. We consider this a likely possibility, however, it requires further research due to

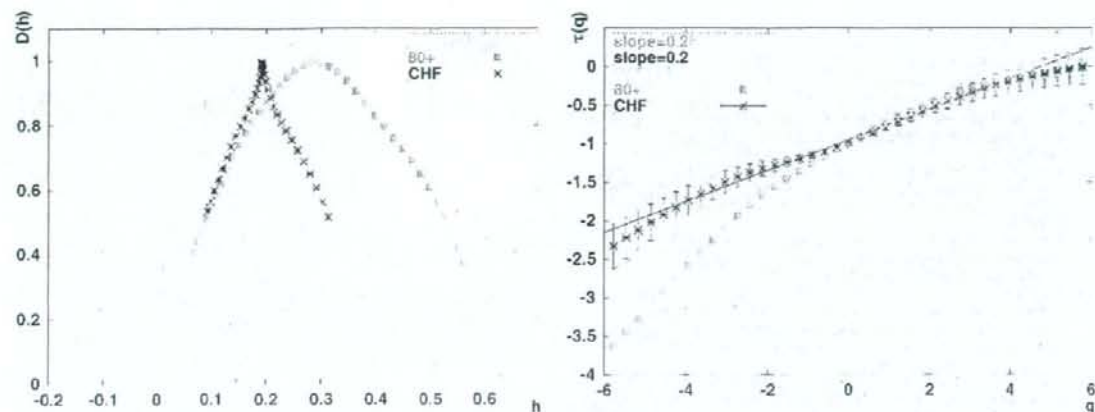


Fig. 6. Singularity spectra  $D(h)$ , together with the  $\tau(q)$  spectra of moments of the partition function  $Z_q(s)$ , for the 80+ healthy subjects and for the PAF and the "simulated autonomic aging" group (PAF + PD) of patients. For reference, the CHF spectrum is also outlined [11].

the limited number of patients in the present study. If verified, this might provide an additional diagnostic window for this prevalent disorder.

## VI. CONCLUSION

The systematic increase in long-range correlation and preserved multifractality of heart rate dynamics with aging, as well as in large-scale brain stem neurodegenerative disorders with the sympathetic dysfunction, suggest that aging is associated with a lack of SNS function, rather than the sympathetic overexcitation seen in, e.g., CHF, to cope dynamically with various environmental stimuli.

## ACKNOWLEDGMENT

The authors wish to thank S. Sakata, K. Kiyono, N. Aoyagi, and K. Saito for their help and discussions.

## REFERENCES

- [1] C. K. Peng, J. Mietus, J. M. Hausdorff, S. Havlin, H. E. Stanley, and A. L. Goldberger, "Long-range anticorrelations and non-Gaussian behavior of the heartbeat," *Phys. Rev. Lett.*, vol. 70, pp. 1343–1346, 1993.
- [2] Y. Yamamoto and R. L. Hughson, "On the fractal nature of heart rate variability in humans: effects of data length and  $\beta$ -adrenergic blockade," *Am. J. Physiol.*, vol. 266, pp. R40–R49, 1994.
- [3] P. C. Ivanov, L. A. N. Amaral, A. L. Goldberger, S. Havlin, M. G. Rosenblum, Z. R. Struzik, and H. E. Stanley, "Multifractality in human heart rate dynamics," *Nature*, vol. 399, pp. 461–465, 1999.
- [4] L. A. N. Amaral, P. C. Ivanov, N. Aoyagi, I. Hidaka, S. Tomono, A. L. Goldberger, H. E. Stanley, and Y. Yamamoto, "Behavioral-independent features of complex heartbeat dynamics," *Phys. Rev. Lett.*, vol. 86, pp. 6026–6029, 2001.
- [5] U. Frisch, *Turbulence*, 1st ed. Cambridge, U.K.: Cambridge Univ. Press, 1995.
- [6] S. Ghoshghaie, W. Breymann, J. Peinke, P. Talkner, and Y. Dodge, "Turbulent cascades in foreign exchange markets," *Nature*, vol. 381, pp. 767–770, 1996.
- [7] P. Bak, C. Tang, and K. Wiesenfeld, "Self-organized criticality: an explanation of  $1/f$  noise," *Phys. Rev. Lett.*, vol. 59, pp. 381–384, 1987.
- [8] H. E. Stanley, "Scaling, universality, and renormalization: three pillars of modern critical phenomena," *Rev. Mod. Phys.*, vol. 71, pp. S358–S366, 1999.
- [9] J. P. Sethna, K. A. Dahmen, and C. R. Myers, "Crackling noise," *Nature*, vol. 410, pp. 242–250, 2001.
- [10] Y. Yamamoto, Y. Nakamura, H. Sato, M. Yamamoto, K. Kato, and R. L. Hughson, "On the fractal nature of heart rate variability in humans: effects of vagal blockade," *Am. J. Physiol.*, vol. 269, pp. R830–R837, 1995.
- [11] Z. R. Struzik, J. Hayano, S. Sakata, S. Kwak, and Y. Yamamoto, "1/f scaling in heart rate requires antagonistic autonomic control," *Phys. Rev. E*, vol. 70, 2004.
- [12] L. A. Lipsitz and A. L. Goldberger, "Loss of 'complexity' and aging: Potential applications of fractal and chaos theory to senescence," *JAMA*, vol. 267, pp. 1806–1809, 1992.
- [13] A. D. Jose and D. Collison, "The normal range and determinants of the intrinsic heart rate in man," *Cardiovasc. Res.*, vol. 4, pp. 160–167, 1970.
- [14] T. Opthof, "The normal range and determinants of the intrinsic heart rate in man," *Cardiovasc. Res.*, vol. 45, pp. 177–184, 2000.
- [15] M. Bursztyjn, M. Bresnahan, I. Gavras, and H. Gavras, "Effect of aging on vasopressin, catecholamines, and  $\alpha_2$ -adrenergic receptors," *J. Am. Geriatrics Soc.*, vol. 38, pp. 628–632, 1990.
- [16] D. C. Shannon, D. W. Carley, and H. Benson, "Aging of modulation of heart rate," *Am. J. Physiol.*, vol. 253, pp. H874–H877, 1987.
- [17] J. B. Schwartz, W. J. Gibb, and T. Tran, "Aging effects on heart rate variability," *J. Gerontol.*, vol. 46, pp. M99–M106, 1991.
- [18] K. Jensen-Urstad, N. Storek, F. Bouvier, M. Ericson, L. E. Lindblad, and M. Jensen-Urstad, "Heart rate variability in healthy subjects is related to age and gender," *Acta Physiol. Scand.*, vol. 160, pp. 235–241, 1997.
- [19] C. Fukusaki, K. Kawakubo, and Y. Yamamoto, "Assessment of the primary effect of aging on heart rate variability in humans," *Clin. Auton. Res.*, vol. 10, pp. 123–130, 2000.
- [20] A. Malliani, M. Pagani, F. Lombardi, and S. Cerutti, "Cardiovascular neural regulation explored in the frequency domain," *Circulation*, vol. 84, pp. 482–492, 1991.
- [21] J. P. Saul, "Beat-to-beat variations of heart rate reflect modulation of cardiac autonomic outflow," *News Physiol. Sci.*, vol. 5, pp. 32–37, 1990.
- [22] D. T. Kaplan, M. I. Furman, S. M. Pincus, S. M. Ryan, L. A. Lipsitz, and A. L. Goldberger, "Aging and the complexity of cardiovascular dynamics," *Biophys. J.*, vol. 59, pp. 945–949, 1991.
- [23] N. Iyengar, C. K. Peng, R. Morin, A. L. Goldberger, and L. A. Lipsitz, "Age-related alterations in fractal scaling of cardiac interbeat interval dynamics," *Am. J. Physiol.*, vol. 271, pp. R1078–R1084, 1996.
- [24] S. M. Pikkujämsä, T. H. Mäkitallio, L. B. Sourander, I. J. Riihää, P. Puukka, J. Skyttä, C. K. Peng, A. L. Goldberger, and H. V. Huikuri, "Cardiac interbeat interval dynamics from childhood to senescence. Comparison of conventional and new measures based on fractals and chaos theory," *Circulation*, vol. 100, pp. 393–399, 1999.
- [25] M. G. Kienzel, D. W. Ferguson, C. L. Birkett, G. A. Myers, W. J. Berg, and D. J. Mariano, "Clinical, hemodynamic and sympathetic neural correlates of heart rate variability in congestive heart failure," *Am. J. Cardiol.*, vol. 69, pp. 761–767, 1992.
- [26] M. Elam, Y. B. Sverrisdottir, D. M. B. Rundqvist, B. G. Wallin, and V. G. Macefield, "Pathological sympathetic excitation: how is it achieved?," *Acta Physiol. Scand.*, vol. 177, pp. 405–411, 2003.
- [27] J. P. Saul, Y. Arai, R. D. Berger, L. S. Lilly, W. S. Colucci, and R. J. Cohen, "Assessment of autonomic regulation in chronic congestive heart failure by heart rate spectral analysis," *Am. J. Cardiol.*, vol. 61, pp. 1292–1299, 1988.



- [28] D. R. Oppenheimer, "Lateral horn cells in progressive autonomic failure," *J. Neurol. Sci.*, vol. 46, pp. 393-404, 1980.
- [29] M. R. Matthews, "Autonomic ganglia and preganglionic neurons in autonomic failure," in *Autonomic Failure*, 4th ed., C. J. Mathias and R. Bannister, Eds. Oxford, U.K.: Oxford Univ. Press, 1999, pp. 329-339.
- [30] S. Sakata, J. Hayano, S. Mukai, A. Okada, and T. Fujinami, "Aging and spectral characteristics of the nonharmonic component of 24-h heart rate variability," *Am. J. Physiol.*, vol. 276, pp. R1724-R1731, 1999.
- [31] N. Aoyagi, K. Ohashi, S. Tomono, and Y. Yamamoto, "Temporal contribution of body movement to very long-term heart rate variability in humans," *Am. J. Physiol. Heart Circ. Physiol.*, vol. 278, pp. H1035-H1041, 2000.
- [32] C. K. Peng, S. Havlin, H. E. Stanley, and A. L. Goldberger, "Quantification of scaling exponents and crossover phenomena in nonstationary heartbeat time series," *Chaos*, vol. 5, pp. 82-87, 1995.
- [33] A. L. Goldberger, L. A. N. Amaral, L. Glass, S. Havlin, J. M. Hausdorff, P. C. Ivanov, R. G. Mark, J. E. Mietus, G. B. Moody, C. K. Peng, and H. E. Stanley, "PhysioBank, PhysioToolkit, and PhysioNet: components of a new research resource for complex physiologic signals," *Circulation*, vol. 101, pp. e215-e220, 2000.
- [34] J. F. Muzy, E. Bacry, and A. Arneodo, "The multifractal formalism revisited with wavelets," *Int. J. Bifurc. Chaos*, vol. 4, pp. 245-302, 1994.
- [35] T. Vicsek, *Fractal Growth Phenomena*, 2nd ed, Singapore: World Scientific, 1993.
- [36] K. P. Davy, D. R. Seals, and H. Tanaka, "Augmented cardiopulmonary and integrative sympathetic baroreflexes but attenuated peripheral vasoconstriction with age," *Hypertension*, vol. 32, pp. 298-304, 1998.
- [37] A. M. Palmer and S. T. DeKosky, "Monoamine neurons in aging and Alzheimer's disease," *J. Neural Transmission*, vol. 91, pp. 135-159, 1993.
- [38] D. A. Bennet, L. A. Beckett, A. M. Murray, K. M. Shannon, C. G. Goetz, D. M. Pilgrim, and D. A. Evans, "Prevalence of parkinsonian signs and associated mortality in community population of older people," *N. Engl. J. Med.*, vol. 334, pp. 71-76, 1996.
- [39] C. Zarow, S. A. Lyness, J. A. Mortimer, and H. C. Chui, "Neuronal loss is greater in the locus coeruleus than nucleus basalis and substantia nigra in Alzheimer and Parkinson diseases," *Arch. Neurol.*, vol. 60, pp. 337-341, 2003.
- [40] S. Orimo, E. Ozawa, S. Nakade, T. Sugimoto, and H. Mizusawa, "<sup>123</sup>I-metaiodobenzylguanidine myocardial scintigraphy in Parkinson's disease," *J. Neurol. Neurosurg. Psych.*, vol. 67, pp. 189-194, 1999.



**Junichiro Hayano** graduated from Nagoya City University Medical School, Nagoya, Japan, and received the M.D. degree in 1980. From 1981 to 1983, he received residency training in psychosomatic medicine at Kyushu University School of Medicine, Fukuoka, Japan. He received the Ph.D. degree (Dr. of Medical Science) in 1988 from Nagoya City University Graduate School of Medical Sciences on the basis of a thesis on the "Assessment of autonomic nervous functions by heart rate variability."

From 1990 to 1991, he worked as a visiting associate at the Behavioral Medicine Research Center, Duke University Medical Center, Durham, NC, mainly on signal processing for ambulatory electrocardiography. In 1984, he was granted a faculty position at Nagoya City University Medical School and has been a Professor of Medicine at Nagoya City University Graduate School of Medical Sciences since 2003. His current interests are applications of dynamic electrocardiography and ambulatory monitoring to clinical cardiology and cardiovascular physiology.



**Rika Soma** received the Ph.D. degree from the University of Tokyo, Tokyo, Japan, in 1996.

From 1997 to 1999, she worked as a research associate at the University of Tsukuba, Tsukuba, Japan. She is currently a postdoctoral researcher at the University of Tokyo. Her fields of interest include the modification of the cardiovascular control system by vestibular stimulation in humans.



**Shin Kwak** was born in Tokyo, Japan, in 1951. He received the M.D. degree from the University of Tokyo, Tokyo, in 1977. He received the Ph.D. degree in medical science from the University of Tokyo in 1984.

In 1984, he got a faculty position at the Department of Neurology, University of Tokyo Hospital. From 1986 to 1987, he worked as a guest scientist at Friedrich-Mischer Institut in Basel. He has been a Full Associate Professor at the Department of Neurology, Graduate School of Medicine, the University of Tokyo since 1997, where he is seeing patients, teaching undergraduate and graduate students, and researching on neurodegenerative diseases. His current interests lie in elucidating the pathogenic mechanism and developing specific therapeutic strategy for amyotrophic lateral sclerosis where he found that RNA editing of AMPA receptor is deficient.

Dr. Kwak was board certified in neurology in 1981.



**Zbigniew R. Struzik** received the M.S. degree in technical physics from the Technical University of Warsaw, Warsaw, Poland, in 1986, and the Doctor of Science degree from the University of Amsterdam, Amsterdam, The Netherlands, in 1996.

Between 1997 and 2003, he worked at the Center for Mathematics and Computer Science (CWI), Amsterdam. His scientific work contributed to the amalgamation of (multi-)fractal analysis, wavelet analysis and time series data mining. He is currently working as an Associate Research Professor at the University

of Tokyo, Japan. His research interests include (multi-)fractals, complex systems, time series processing and mining, and, in particular, applications of the wavelet transformation. He is on the editorial board of the *Fractals Journal*, on the reviewers' board of the *Data and Knowledge Engineering Journal* and is a Database Expert Systems Applications (DEXA) program committee member.



**Yoshiharu Yamamoto** was born in Tokyo, Japan, in 1960. He received the Ph.D. degree in education from the University of Tokyo, Tokyo, Japan, in 1990.

From 1989 to 1993, he was working as a Postdoctoral Researcher at the Department of Kinesiology, University of Waterloo, Waterloo, ON, Canada, mainly on biosignal processing for human cardiovascular physiology. In 1993, he got a faculty position at the Graduate School of Education, the University of Tokyo, and has been a Full Professor at the Educational Physiology Laboratory, Graduate School of Education, the University of Tokyo since 2000, where he is teaching and researching physiological bases of health sciences and education. His current interests lie in biomedical signal processing, nonlinear and statistical bio-dynamics, and regulatory physiology. See <http://www.p.u-tokyo.ac.jp/~yamamoto/yoyeve/yycve.html>, for details.

## Transferrin localizes in Bunina bodies in amyotrophic lateral sclerosis

Yuji Mizuno · Masakuni Amari · Masamitsu Takatama ·  
Hitoshi Aizawa · Ban Mihara · Koichi Okamoto

Received: 21 June 2006 / Revised: 13 July 2006 / Accepted: 13 July 2006 / Published online: 5 August 2006  
© Springer-Verlag 2006

**Abstract** Transferrin, an iron-binding protein, plays an important role in the transport and delivery of circulating ferric iron to the tissues. Amyotrophic lateral sclerosis (ALS) is characterized by the presence of Bunina bodies, skein-like inclusions, Lewy body-like inclusions/round inclusions, and basophilic inclusions in the remaining anterior horn cells in the spinal cord. We examined transverse paraffin sections of lumbar spinal cords from 12 ALS cases including two ALS with dementia and two ALS with basophilic inclusions, using antibodies to human transferrin. The results demonstrated that transferrin localized in Bunina bodies and some of the basophilic inclusions. In contrast, skein-like inclusions and Lewy body-like inclusions or round inclusions did not show obviously detectable transferrin immunoreactivities. Our findings suggest that although the mechanisms underlying transferrin accumulation in Bunina bodies and basophilic inclusions are unknown,

transferrin could be involved in forming these inclusions. Furthermore, following cystatin C, transferrin is the second protein that localizes in the Bunina bodies.

**Keywords** Amyotrophic lateral sclerosis · Basophilic inclusions · Bunina bodies · Cystatin C · Transferrin

### Introduction

Amyotrophic lateral sclerosis (ALS) is neuropathologically characterized by loss of motor neurons and occurrence of Bunina bodies [21, 23], skein-like inclusions (SLI) [9], and Lewy body-like inclusions (LBLI) [6, 7, 14] in the remaining anterior horn cells of the spinal cord. Bunina bodies [21] ranging from 2 to 5  $\mu\text{m}$  are present alone or in series in anterior horn cells in ALS, and LBLI [7] are more often seen in familial ALS than in sporadic ALS. With respect to the definition of LBLI, some authors have suggested that the name of LBLI should be used only in familial cases [7] and when an appearance similar to LBLI is observed in sporadic ALS cases, the name round inclusions would be better because the components of LBLI are different from those of LBLI-like inclusions. LBLI are indistinguishable from Lewy bodies seen in Parkinson's disease when stained with hematoxylin and eosin (H&E), but they are immunostained with Cu/Zn superoxide dismutase [12] but not  $\alpha$ -synuclein [1], while Lewy bodies are immunohistochemically positive for  $\alpha$ -synuclein [1]. Moreover, ALS with onset before the age of 20 has been reported as sporadic juvenile disease, in which cytoplasmic basophilic inclusions [4] have been observed as one of the characteristic features. Bunina bodies are immunohistochemically positive for cystatin C and ubiquitin-negative, while SLI and LBLI appear as

Y. Mizuno (✉) · K. Okamoto  
Department of Neurology, Gunma University Graduate  
School of Medicine, 3-39-22 Showa-machi,  
Maebashi, Gunma 371-8511, Japan  
e-mail: mizunoy@med.gunma-u.ac.jp

M. Amari · M. Takatama  
Department of Internal Medicine, Geriatrics Research  
Institute and Hospital, 3-26-8 Otomo-machi, Maebashi,  
Gunma 371-0847, Japan

H. Aizawa  
First Department of Internal Medicine,  
Asahikawa Medical College, Asahikawa 078-8510, Japan

B. Mihara  
Institute of Brain and Blood Vessels,  
Mihara Memorial Hospital, 366 Ota-machi,  
Isesaki, Gunma 372-0006, Japan



ubiquitin-positive, tau-negative, cystatin-C-negative, and  $\alpha$ -synuclein-negative. Basophilic inclusions show a globular or irregular-shaped appearance and are occasionally positive for ubiquitin with granular reaction. The mechanism for the formation of cytoplasmic inclusions remains unknown; therefore, elucidation of the main constituents is very important to understand the significance of these inclusions.

Transferrin, an 80-kDa glycoprotein, is an iron-binding plasma protein [2] that is capable of binding two iron atoms per molecule, diferric transferrin. Differing from monoferric transferrin and apotransferrin, diferric transferrin has a high affinity to transferrin receptor, a 180-kDa disulphide-bonded protein dimer of two identical subunits on the cell surface. Once iron-loaded transferrin binds to the transferrin receptor, the receptor–transferrin complex is internalized by endocytosis and the resulting endocytotic vesicle fuses with an acidic compartment. Dissociation of iron from transferrin occurs, and iron enters the cytoplasm. Apotransferrin is released extracellularly and binds more iron [10].

Neurons do not synthesize transferrin, although transferrin is synthesized within the oligodendrocytes [2] and choroid plexus epithelial cells of the third and lateral ventricles [3]. Therefore, plasma proteins like transferrin are thought to reach the neurons by endocytosis [10], the uptake of iron-loaded transferrin via transferrin receptor, or by nerve terminals at the area where the plasma proteins pass the nerve terminal from the blood and then retrograde transport occurs [11, 15, 26]. Large polygonal and pyramidal cells show more transferrin immunoreactivity in the amygdala and brainstem, reflecting the high densities of transferrin receptor on these cells [16]. Liu et al. [11] reported that 90–100% of neurons of the spinal cord as well as their axons of anterior horn cells show strong immunostaining for albumin and moderate to strong staining for transferrin.

Little attention has been paid to transferrin expression in neurodegenerative diseases. To better understand abnormal protein accumulation in the remaining anterior horn cells in ALS, we examined spinal cords from 12 ALS patients including two cases of ALS with dementia (ALS-D) and two cases of basophilic inclusion type of ALS, using antibodies against transferrin. We found that transferrin localized in Bunina bodies and some of the basophilic inclusions, in addition to diffuse cytoplasmic distribution of transferrin in the anterior horn cells.

## Materials and methods

We examined a total of 12 ALS lumbar spinal cords (average patient age: 59.3 years old, sex: 6 males, 6

females) including two ALS-D cases (64-year-old female and 46-year-old male) and two ALS cases demonstrating basophilic inclusions (24- and 27-year-old females), in addition to samples from five non-ALS patients with Parkinson's disease, Alzheimer's disease, or Creutzfeldt–Jakob disease. Spinal cord tissues were all obtained from institutes and universities. In all cases, the autopsies were performed in accordance with established procedures and the samples were used in this study after obtaining informed consent from the family of each patient. All patients were definitively diagnosed based on clinical and light microscopic findings of the spinal cords and some of the data from several patients were previously reported elsewhere [4, 13]. Spinal cords were fixed with 4% paraformaldehyde in phosphate-buffered solution (PBS) (pH 7.4) and embedded in paraffin. Five micrometer thick transverse paraffin sections were prepared for immunohistochemistry, which was carried out using a rabbit polyclonal anti-human transferrin antibody (1:6,000; DakoCytomation, Glostrup, Denmark), a goat polyclonal anti-human transferrin antibody (1:20,000; MP Biomedicals, Ohio, USA), and rabbit polyclonal anti-albumin (1:5,000; DakoCytomation), anti-prealbumin (1:5,000; DakoCytomation), and anti-orosomucoid antibodies (1:2,000; DakoCytomation). For enhancement, autoclave treatment for 5 min was performed when anti-transferrin antibody was used. Sections were blocked in normal horse serum for 30 min at room temperature, then labeled with the first antibody at 4°C overnight, washed in PBS for 30 min, incubated with the second antibody provided by Histofine SAB-PO kit (Nichirei, Tokyo, Japan), washed in PBS for 30 min, and finally visualized by the avidin–biotin–peroxidase method. Observation was performed using an Olympus BX50 microscope.

Specificity of the transferrin staining was confirmed by preabsorption of the antibody for 1 h at 4°C with 100  $\mu$ M human transferrin (Sigma).

For Bunina bodies, Lewy body-like inclusions, and basophilic inclusions, H&E staining was initially performed to observe the locations of these structures. After photographing these findings, we removed the cover glasses from the slides in xylene, decolorized the specimens in alcohol, and performed the same process for transferrin immunostaining.

## Results

In general, the cytoplasm and processes of the anterior horn cells showed almost homogeneously transferrin-positive immunoreactivities in ALS and non-ALS



cases (Fig. 1), although the intensities differed in each anterior horn cell, ranging from weak staining to strong staining. In addition, small cells were seen between and around the anterior horn cells, in which transferrin-positive products were detected adjacent to the nuclei (arrows in Fig. 1). Transferrin immunoreactivity was confined to a thin rim of perinuclear cytoplasm in a cap-like fashion, suggesting that these cells were oligodendrocytes (data not shown), as previously reported [2]. Little differences of transferrin immunoreactivity among each anterior horn cell were seen in ALS, ALS-D, the basophilic type of ALS, and non-ALS cases.

In addition to weak staining of transferrin within the cytoplasm, small transferrin-positive circular structures were observed in the cytoplasm of anterior horn cells in all ALS cases except one sporadic case (Fig. 2a). The periphery of their structures showed strong immunoreactivity compared to that at the center. The number of transferrin-positive structures varied in each spinal cord section. To determine whether the transferrin-positive reactions were specific, a serial section was immunostained after preabsorption of anti-transferrin antibody with human transferrin for 1 h at 4°C. The finding showed that transferrin-positive staining disappeared (Fig. 2b), indicating that the reaction was true.

Since circular transferrin-positive staining likely corresponded to Bunina bodies, H&E staining was performed initially to confirm where those structures showing eosinophilic inclusions were located (Fig. 3a, c). After photographing the Bunina bodies shown by H&E staining, immunohistochemistry for

transferrin was examined on the same section. The result showed that transferrin immunoreactivities (Fig. 3b, d) were seen at the same location as Bunina bodies, indicating that transferrin was co-localized with Bunina bodies and that Bunina bodies were related to transferrin. Using a different anti-human transferrin antibody purchased from MP Biomedicals, Bunina bodies were similarly shown as transferrin positive (data not shown). Bunina bodies were not immunoreactive for other plasma proteins such as albumin, prealbumin, and orosomucoid (data not shown).

Lewy body-like inclusions or round inclusions showing an eosinophilic core with a peripheral halo appearance were detected on H&E staining in a sporadic ALS case (Fig. 4a, c). After the H&E stained section was decolorized by alcohol, transferrin staining was performed, showing a slightly stronger immunoreaction for Lewy body-like inclusions at the core than in the cytoplasm (Fig. 4b, d). However, the staining level was obviously weak compared to that of Bunina bodies.



**Fig. 1** Transferrin immunoreactivity in anterior horn cells. Cytoplasm and processes were diffusely transferrin positive. Small cells showing transferrin-positive immunoreactivity were scattered around the anterior horn cells (arrows). Scale bar: 20  $\mu$ m

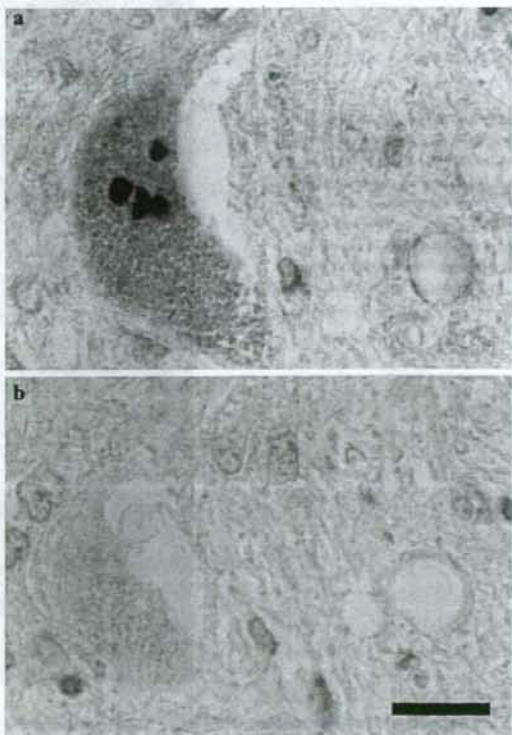


**Fig. 2** Transferrin immunoreactivity in small circular structures. **a** Immunostaining for transferrin. **b** Immunostaining for transferrin preabsorbed with human transferrin. Transferrin immunostaining was obviously specific. Scale bar: 20  $\mu$ m



**Fig. 3** Transferrin immunoreactivity in Bunina bodies. **a, c** H&E staining. **b, d** Immunostaining for transferrin. Bunina bodies (**a, c**) were transferrin positive. The presence of Bunina bodies was confirmed with H&E staining (**a, c**), and the same section was examined with anti-transferrin antibody (**b, d**). Scale bar: 20  $\mu$ m

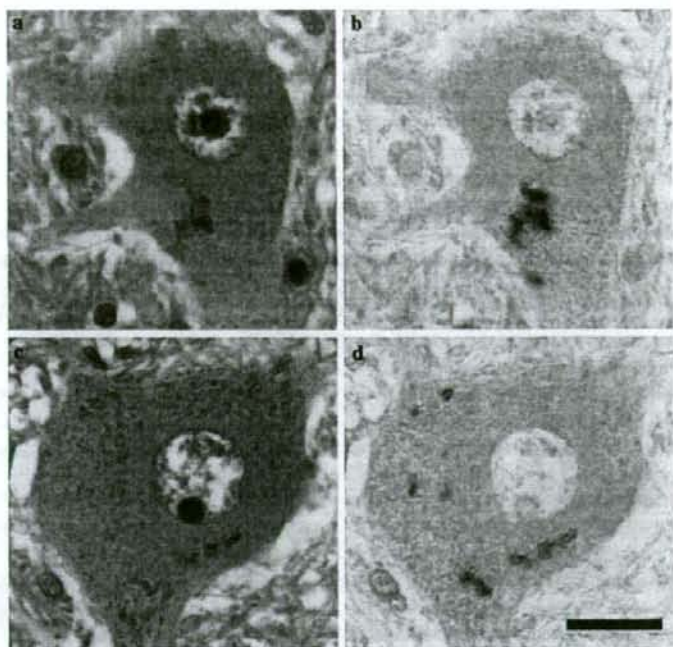
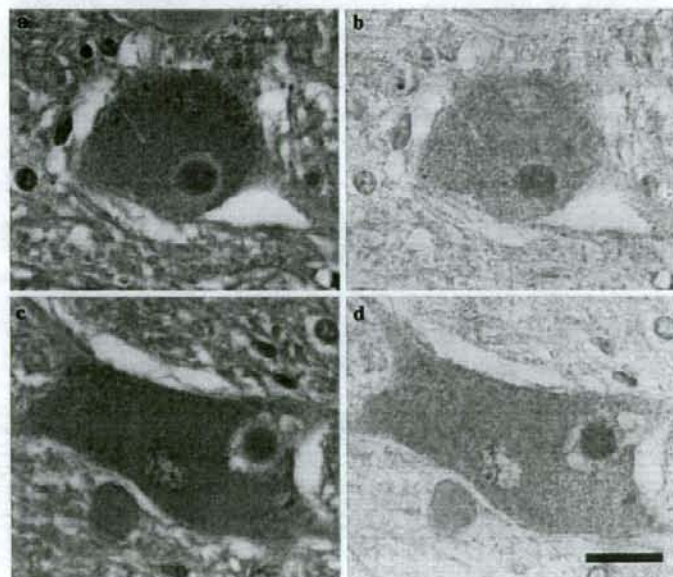


**Fig. 4** Transferrin immunoreactivity for Lewy body-like inclusions. **a, c** H&E staining. **b, d** Immunostaining for transferrin. The presence of Lewy body-like inclusions was confirmed with H&E staining (**a, c**), and the same section was examined with anti-transferrin antibody (**b, d**). Scale bar: 20  $\mu$ m



Confirming the horseshoe-shaped, multilobulated, globular, tubular or spheroid inclusions that appeared basophilic in the cytoplasm of anterior horn cells on H&E staining, which were recognized as basophilic inclusions (BI), (Fig. 5a, c, e, g), we examined 15 BI

detected in two ALS cases to determine whether the structures were positive for transferrin. The findings demonstrated that immunoreactive patterns for transferrin were roughly classified into three types. Five obvious transferrin-positive BI were detected among

15 inclusions (Fig. 5b, d), although the immunoreactivity was heterogeneous not homogeneous. Furthermore, detectable but weak heterogeneous immunostaining was observed in five inclusions (Fig. 5f). There were five BI that were almost transferrin negative (Fig. 5h).

We observed numerous skein-like inclusions showing p62-positive staining of sections from ALS cases, however, these inclusions were transferrin negative in the adjacent sections (data not shown). Furthermore, other structures such as granulovacuolar degeneration and neurofibrillary tangles in Alzheimer's disease were not immunostained for transferrin (data not shown).

## Discussion

Among comparatively ALS-specific structures such as Bunina bodies [21, 23], skein-like inclusions [9], Lewy body-like inclusions or round inclusions [6, 7, 14] and basophilic inclusions [4], Bunina bodies showed obvious immunoreactivity for transferrin. The origin of Bunina bodies is unknown, however, several authors have reported that it could be related to autophagic vacuole [5] and Golgi apparatus [19, 22]. Recently, we found that skein-like inclusions, LBLI or round inclusions, and some of the basophilic inclusions in the remaining anterior horn cells were p62 positive [13], while Bunina bodies were negative for p62. These findings are interesting because skein-like inclusions, LBLI or round inclusions, and some of the basophilic inclusions are immunoreactive for ubiquitin.

Cystatin C is a member of a super family of protease inhibitors, and involved in processes such as tumor invasion and metastasis, inflammatory processes, and some neurological diseases [25]. Okamoto et al. [23] reported that cystatin C localizes in Bunina bodies of ALS cases. In addition to the increase of 14-3-3 proteins in the cerebrospinal fluid (CSF), cystatin C could also be one of the interesting diagnostic markers of sporadic Creutzfeldt-Jakob disease [24]. In contrast, cystatin C in the CSF has been found to be down-regulated in patients with leptomeningeal metastasis [18], Guillain-Barre syndrome [17], or chronic inflammatory demyelinating polyneuropathy [17]. Transferrin is a major glycoprotein playing an important role in the transport of circulating ferric iron and its delivery to tissues that express surface transferrin receptor. The presence of unusual glycosylated isoforms of transferrin and the specific enrichment and oxidation of transferrin isoforms has been reported in Alzheimer's disease (AD) plasma [29]. Moreover, Piubelli et al. [24] demonstrated that transferrin is fivefold up-regulated

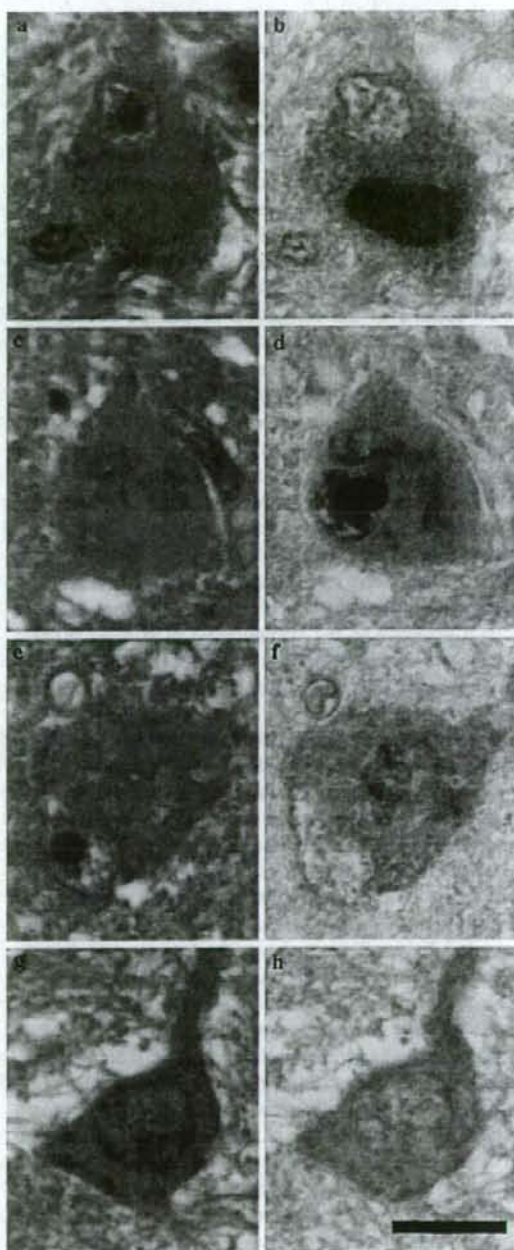


**Fig. 5** Transferrin immunoreactivity for basophilic inclusions. **a, c, e, g** H&E staining. **b, d, f, h** Immunostaining for transferrin. Basophilic inclusions showed strongly transferrin-positive (**b, d**), weak (**f**) and negative (**h**) reaction. The presence of these structures was confirmed with H&E on same sections. Scale bar: 20  $\mu$ m